SAND2015-2251R

Draft Geologic Disposal Requirements Basis for STAD Specification

Fuel Cycle Research & Development

Prepared for
U.S. Department of Energy
Nuclear Fuels Storage and Transportation Planning Project

A. Ilgen, C. Bryan, and E. Hardin
Sandia National Laboratories
March 25, 2015

FCRD-NFST-2013-000723
SAND2014-xxxxx

Sandia National Laboratories is a multi-program laboratory managed and operated by Sandia Corporation, a wholly owned subsidiary of Lockheed Martin Corporation, for the U.S. Department of Energy's National Nuclear Security Administration under contract DE-AC04-94AL85000.

SUMMARY

This document provides supporting technical rationale in draft form as input for: *STAD Performance Specification Requirements Rationale* (planned to be issued as FCRD-NFST-2015-000106). The supporting rationale addresses those parts of the storage, transportation and disposal (STAD) canister performance specification that pertain to geologic disposal. These parts include service lifetime, repository thermal performance, postclosure criticality, and materials selection.

Each draft performance specification is presented, and those pertaining to geologic disposal are elaborated with brief sections labeled Rationale. More detail is provided in appendices that address: long-term performance of borated stainless steel, use of borated stainless steel in existing designs, recommendations for additional corrosion studies, stress corrosion cracking of canister shell materials, and a generic postclosure safety case for STAD canisters.

CONTENTS

SUMMARY iii

ACRONYMS viii

1. INTRODUCTION 1

2. (RESERVED) ..... **Error! Bookmark not defined.**

3. PERFORMANCE REQUIREMENTS 1
   - 3.1 STAD Canister 1
     - 3.1.1 General 1
     - 3.1.2 Structural 3
     - 3.1.3 Thermal 3
     - 3.1.4 Dose and Shielding 6
     - 3.1.5 Criticality 6
     - 3.1.6 Confinement and Containment 8
     - 3.1.7 Operations 9
     - 3.1.8 Materials 9
     - 3.1.9 Security 10

4. REFERENCES 11

Appendix A. Borated vs. Non-Borated Stainless Steel: Corrosion Rates and Mechanisms 16

Appendix B. Welding-Induced Alteration of Borated Stainless Steel and Methods for Weld Mitigation 20

Appendix C. Review of the Use of Borated Stainless Steel in Existing Designs. 21

Appendix D. Recommendations for Additional Corrosion Studies on Borated Stainless Steel 24

Appendix E. Stress Corrosion Cracking of Spent Nuclear Fuel Interim Storage Canisters 26

Appendix F. Generic Case for Postclosure Safety of STAD Canisters 35

FIGURES

Figure E-1. Criteria for SCC initiation and growth. 27

Figure E-2. Relationship between canister surface temperature, relative humidity, and RH at the canister surface. 28

Figure E-3. Aggregates of sea-salts (NaCl + Mg-SO_4) collected from the surface of an in-service SNF storage canister at Diablo Canyon 29

Figure E-4. Predicted weld residual stress profiles in canister weld regions (NRC 2013). Left-circumferential weld; right-longitudinal weld. 31

Figure E-5. SCC propagation rates for atmospheric corrosion of 304SS and 316SS. BM –base metal; W–weld sample; SA–solution annealed; S–sensitized. Bars represent

reported ranges (if more than one), while symbols represent average values. Time to failure corresponds to the time required to penetrate a 0.625" thick canister wall. 34
Figure F-1. Conceptual model for generic repository waste isolation analysis (after Freeze et al., 2013). 36
Figure F-2. Calculated dose for a generic salt repository (after Freeze et al., 2013)..... 36
Figure F-3. Calculated dose for a generic clay/shale repository (after Freeze et al., 2013). 37
Figure F-4. Calculated dose for a generic crystalline rock repository (after Freeze et al., 2013). 37
Figure F-5. High-reactivity model geometry (upper) and neutron multiplication factor (k_{eff}) as a function of NaCl salt concentration, for different fuel types (lower). 41
Figure F-6. Event-tree logic for a stylized criticality screening analysis. 42
Figure F-7. Event-tree logic for a stylized criticality screening analysis of the inadvertent human intrusion scenario. 42

TABLES

Table 1. Postclosure Thermal Conditions for Canister Heat Dissipation 4
Table 2. Disposal Overpack Temperature Drop for Postclosure Thermal Conditions 5
Table 3. Maximum Power Levels for STAD Canisters at a Repository 6
Table A-1. Corrosion rates of borated and non-borated stainless steels 19
Table B-1. Proposed Representative Groundwater Chemical Compositions 25
Table F-1. Summary of Postclosure Dose Standards Based on 10 CFR Part 63. 40

ACRONYMS

ASTM	American Society for Testing and Materials
BWR	Boiling Water Reactor
CFR	Code of Federal Regulation
DOE	US Department of Energy
DPC	Dual-Purpose Canister
FCRD	Fuel Cycle Research and Development
HLW	High-Level Radioactive Waste
ISFSI	Independent Spent Fuel Storage Installation
ISF	Interim Storage Facility
ISG	Interim Staff Guidance
LLW	Low-Level Radioactive Waste
MPC	Multipurpose Canister
NFST	Nuclear Fuel Storage and Transportation
NRC	U.S. Nuclear Regulatory Commission
PWR	Pressurized Water Reactor
R&D	Research and Development
SKB	Swedish Nuclear Fuel and Waste Management Company
SNF	Spent Nuclear Fuel
STAD	Standardized Transportation, Aging, and Disposal [canister]
TAD	Transportation, Aging, and Disposal [canister]
UFD	Used Fuel Disposition
WP	Waste Package

DRAFT GEOLOGIC DISPOSAL REQUIREMENTS BASIS FOR STAD SPECIFICATION

1. INTRODUCTION

This document provides the basis for requirements in the current version of *Performance Specification for Standardized Transportation, Aging, and Disposal Canister Systems*, (FCRD-NFST-2014-0000579) that are driven by storage and geologic disposal considerations. Performance requirements for the Standardized Transportation, Aging, and Disposal (STAD) canister are given in Section 3.1 of that report. Here, the requirements are reviewed and the rationale for each provided. Note that, while FCRD-NFST-2014-0000579 provides performance specifications for other components of the STAD storage system (e.g. storage overpack, transfer and transportation casks, and others), these have no impact on the canister performance during disposal, and are not discussed here.

2. (RESERVED)

3. PERFORMANCE REQUIREMENTS

3.1 STAD Canister

In the sections that follow, all of the specifications and subsections of Section 3.1 of the STAD *Performance Specification* are provided. For those specifications that are based at least in part on geologic disposal requirements, the disposal-based rationale is provided. For specifications with no disposal basis, rationale is not provided in this document.

3.1.1 General

1. *The 10 CFR Part 72 and 10 CFT Part 71 requirements apply to the loaded STAD canister in a transportation or storage overpack, respectively. The guidance in NUREG-1536 Rev 1 and NUREG-1567 for storage, and in NUREG-1617 for transportation, provide approaches that have been accepted by the NRC staff in the past, and are used as requirements in this Performance Specification document. Applicants can use alternative approaches if the previously accepted approaches are not applicable to the particular circumstances of the STAD canister. Additionally, the loaded STAD canister exists outside an overpack for short periods of time, and this Performance Specification document indicates requirements applicable during that time.*

2. *The design lifetime of the STAD canister shall be 150 years from the time the canister is loaded with SNF to the time the canister is loaded into a waste package, that could potentially include multiple dry storage and transportation cycles. It is acceptable to use aging management protocols necessary to ensure continued compliance with applicable requirements, and/or engineered measures to control the canister storage environment.*

   Rationale: Selection of a 150-year service life for STAD canisters (as defined above) is tied to assumptions used in previous work, regulatory considerations, and documented descriptions of alternative disposal concepts. It is recognized that absolute assurances for 150-year service life cannot be made, but rather that projected performance is based on engineering judgement, qualified by available data on material performance in potential service environments.

   A previous study that evaluated technical feasibility of direct disposal of SNF in dual-purpose canisters (DPCs), adopted an assumption that the combined durations of surface storage and repository operation would not be evaluated beyond 150 years to limit any

additional assumptions about long-term stability of institutions responsible for waste management (Hardin and Howard, 2013). This assumption is comparable to 40 CFR 191.14(a) which states "...performance assessments that assess isolation of the wastes from the accessible environment shall not consider any contributions from active institutional controls for more than 100 years after disposal." Following this logic, there should be a comparable limit on the duration that STAD canisters are stored, during which active institutional controls would be relied on to monitor containment and to ensure security, safeguards, and ultimate disposal.

The 150-year service lifetime provides ample time for STAD canisters to cool before packaging and emplacement in a repository. For some disposal concepts, especially those involving use of clay-based buffer or backfill materials, this cooling time would be essential (see emplacement power limits for Cases 1 to 3 and 11 to 16 in Hardin and Kalinina, 2015). For other concepts such as the salt repository cases and hard rock unsaturated/unbackfilled cases disposal could occur much sooner even for higher burnup SNF (compared to assembly aging-burnup power curves in Figure 2 of Hardin et al., 2013; Cases 4 to 10 in Hardin and Kalinina, 2015).

3. *The STAD canister is required to have a circular cross section (in the plane perpendicular to the canister's long axis).*

   Rationale: The specification for a cylindrical canister external geometry is driven by the need to place STAD canisters into overpacks for storage, transportation, and disposal. Current designs for spent fuel dry storage and transportation casks (Greene et al., 2013) and waste packages for geologic disposal (DOE, 2008b, Section 1.5.2) call for cylindrical geometry.

4. *The STAD canister design shall accommodate the varying lengths of the current inventory of SNF, by using a flexible design that can be fabricated at several lengths. The design must be integrated with storage overpack and transportation overpack designs, and with length-handling capabilities at existing reactor facilities.*

5. *The canister-lifting feature shall be incorporated into the canister top lid and shall not protrude beyond the canister side-walls.*

6. *The STAD canister, along with its STC, shall be compatible with load limits and crane-lifting capacities at existing reactor sites.*

7. *The capacity of the small STAD canister shall be either four PWR SNF assemblies or nine BWR SNF assemblies. The outside diameter of the small PWR and BWR canisters must be the same.*

8. *The capacity of the medium STAD canister shall be either 12 PWR SNF assemblies or 32 BWR SNF assemblies. The outside diameter of the medium PWR and BWR canisters must be the same*

9. *The capacity of the large STAD canister shall be either 21 PWR SNF assemblies or 44 BWR SNF assemblies. The outside diameter of the large PWR and BWR canisters must be the same.*

10. *The loaded and closed STAD canister shall be capable of being reopened while submerged in a borated or unborated pool.*

11. *A STAD canister for PWR or BWR assemblies shall be limited to accepting SNF with initial enrichment up to 5 wt % U-235 and burnup up to 62.5 GWd/MTU. 10 CFR Parts 71.4 and 72.2 define spent nuclear fuel as having been discharged from the reactor for at least one year. Required cooling (decay) time before loading may be variable based on enrichment, burnup, and assembly design.*

12. *A STAD canister shall be capable of being loaded with SNF from all facilities that are licensed by the NRC and hold a contract with DOE for disposal of SNF.*
13. *All external edges of the STAD canister shall have a minimum radius of curvature of 0.25 in.*
14. *To the extent practicable, projections or protuberances from reasonably smooth adjacent surfaces shall be avoided or smoothly blended into the adjacent smooth surfaces, such that loading into a storage or transportation overpack will be facilitated with a low potential for damage to the interior of the overpack.*
15. *The STAD canister shall be designed to store SNF at a utility site's ISFSI and ISF in either a horizontal or vertical orientation.*
16. *A STAD canister shall be designed to be transportable in a horizontal configuration.*

3.1.2 Structural

1. *The STAD canister shall meet the storage leak criterion accepted in NUREG-1536 Rev 1 with endorsement of ANSI N14.5-97. The STAD canister in conjunction with the transportation overpack must meet the transportation containment criteria accepted in NUREG-1617.*
2. *For storage at an ISFSI or ISF with a site-specific license (as opposed to an ISFSI with a general license), the seismic analysis in NUREG-1567 should consider the probabilistic seismic hazard analysis and performance-based safety assessment guidance in HLWRS-ISG-01 that supplemented the guidance in NUREG-1804 Rev 2, Yucca Mountain Review Plan.*
3. *The STAD canister shall constitute the confinement boundary during storage. 10 CFR Part 72.236 requires redundant sealing of confinement systems for a storage cask. This Performance Specification document assigns that requirement to the STAD canister, requiring dual welded closures.*

Rationale: Items 1 and 3 are in part based on disposal requirements. Although the bulleted items specifically discuss requirements during storage, one rationale for those requirements is to ensure that the canister and enclosed SNF meet requirements for transportation and ultimate disposal. Several recent analyses of the safety performance of long-term interim storage have identified through-penetration of the stainless steel storage canisters by stress corrosion cracking (SCC) at canister weld zones as one of the greatest risks to performance (NWTRB, 2010; EPRI, 2011; Hanson et al., 2012; NRC, 2012). A summary of the current state of knowledge with respect to canister SCC is presented in Appendix E. The leak-tight requirement drives specifications for mitigation of canister welds to reduce the likelihood of canister penetration by SCC, as discussed in Section 3.1.8.

3.1.3 Thermal

1. *SNF cladding temperatures in STAD canisters shall meet applicable limits established in NRC Review Plans and guidance documents. For storage, NUREG-1536 Rev 1, Section 4.4.2, specifies zirconium and stainless steel cladding limits of 400°C for normal conditions of storage and short term loading operations including cask drying and backfilling. NUREG-1536 Rev 1, Section 4.4.2, also provides a cyclic limit during loading, with repeated thermal cycling limited to less than 10 cycles, with cladding temperature variations that are less than 65°C. For off-normal and accident conditions, the limit is 570°C for both types of cladding. For transportation, SFST-ISG-11, Revision 3, Cladding Considerations for the Transportation and Storage of Spent Fuel, affirms these temperature limits.*
2. *To meet repository thermal management objectives, the maximum cladding temperature shall be less than 400°C, given emplacement of a disposal overpack containing a single STAD canister, with the power and surface temperature boundary conditions provided in Table 1. For the purpose of canister*

internal temperature analysis, the canister outer surface temperature may be conservatively assumed to be 3 ℃ hotter than the disposal overpack outer surface temperature.

Table 1. Postclosure Thermal Conditions for Canister Heat Dissipation

Concept	STAD Canister Maximum Postclosure Thermal Power	Canister Maximum Surface Temperature Boundary Condition
Postclosure Conditions for STAD Canister Internal Dissipation		
Small STAD Canister	2,200 W	200°C
Medium STAD Canister	5,500 W	200°C
Large STAD Canister	10,000 W	200°C

Rationale: Cladding temperature limits for STAD canisters during storage, handling, transport, and emplacement at a repository (item 1 above) are based on regulatory guidance (NUREG-1536 Rev. 1 and SFST-ISG-11). Postclosure thermal specifications are based on the same cladding temperature limits. The maximum postclosure power levels (Table 1) correspond to the maximum power at closure (and at emplacement, for Cases 1 to 7) for each STAD canister size, over all of the size-specific disposal concepts described by Hardin and Kalinina (2015).

Postclosure thermal specifications for STAD canisters are derived from: 1) the requirement for maximum cladding temperature of 400°C, and 2) maximum overpack surface temperature (equal to maximum near-field temperature) in the repository after closure. The maximum overpack surface temperature is determined from thermal analysis of the repository environment outside the waste package (Hardin et al., 2012; Hardin, 2013) which was used as basis information for emplacement and closure power limits given by Hardin and Kalinina (2015). The postclosure limiting thermal conditions (Table 1) are intended to control the internal heat dissipation performance of STAD canisters.

The postclosure thermal conditions (Table 1) include two simplifying assumptions. Firstly, thermal resistance of the disposal overpack is neglected. Thus, if the waste package surface temperature (instead of the STAD canister surface) is specified to be 200°C, then the canister surface temperature will actually be slightly greater than 200°C. The difference between canister and overpack surface temperatures can be estimated from the thermal resistance of the overpack. Considering heat conduction across the disposal overpack thickness, the temperature differences are less than 2ºC (Table 2). The differences in Table 2 are calculated for the same cases used to develop Table 1.

Table 2. Disposal Overpack Temperature Drop for Postclosure Thermal Conditions

Canister Capacity (PWR assy.'s)	Case #'s (Hardin and Kalinina, 2015)	Post-closure Power, kW	Waste Package OD, m	Waste Package Length, m	Overpack Wall Thickness, m	Overpack K_{th}, W/m-K	Overpack Heat Flow Area, m^2	ΔT, C
4	4	2.2	0.82	5	0.15	30	11.2	1.0
12	5	5.5	1.02	5	0.15	30	14.8	1.9
21	6	10	1.57	5	0.07	15	27.1	1.7

The second simplification is that near-field temperature variation is neglected for "open" disposal concepts for which an air gap is maintained around waste packages after repository closure, and which include a drip shield (Cases 8, 9 and 10 from Hardin and Kalinina, 2015). The following paragraph is provided for rationale, noting that none of these cases is used as the basis for controlling postclosure thermal conditions in Table 1.

For Cases 8, 9 and 10 (Hardin and Kalinina, 2015) the controlling near-field temperature is a 200°C limit for the host rock at the emplacement drift wall. Between the waste package surface and the drift wall is an air gap of approximately 1 to 2 m, and a metal drip shield which acts as a thermal radiation shield. The response of both was shown previously to result in a temperature drop from the waste package to the drift wall of 10 to 20°C at the time of the waste package peak temperature (BSC, 2008, Section 6.1.4). The combination of overpack temperature drop, plus thermal radiation effects for "open" concepts, tends to increase the STAD canister surface temperature. However, the increase is small compared to the overall magnitude of temperature increases in a repository. In the event that STAD canisters would not meet cladding temperature limits for the conditions identified in Table 1 with addition of ΔT from Table 2 plus the thermal radiation effect, the repository postclosure power values (Table 1) can be reduced.

Thermal limits for preclosure handling, storage, and transportation are also controlled by the cladding peak temperature limits (NUREG-1536 Rev. 1 and SFST-ISG-11, as required in item 1 above). At the repository, waste packages ready for emplacement will have power output as high as those limits noted in Table 3. These power values for clarity because power output during repository operations may be less than during upstream storage and transportation activities. It is likely that with the similarity of repository handling, aging, transport and emplacement equipment to corresponding systems used upstream, that the NUREG-1536 and SFST-ISG-11 limits will be met during repository operations. Note that the 18 kW limit in Table 3 for large STAD canisters is based on previous analysis (BSC, 2008, Sections 1.2.4.4 and 1.3.1).

Table 3. Maximum Preclosure Power Levels for STAD Canisters at a Repository

Preclosure Conditions for STAD Canister Internal Dissipation During Handling/Transport			
	Case # from Hardin and Kalinina (2015)	**Maximum Preclosure Power at the Repository**	
Small STAD Canister	4	2,200 W	Canister surface temperature during preclosure repository storage/ handling/transport/emplacement operations is to-be-determined from analysis that includes the dissipation efficiency of storage/handling/ transport/emplacement containers and equipment used at the repository.
Medium STAD Canister	8, 11, 14	10,000 W	
Large STAD Canister	9, 12, 15	18,000 W	

3.1.4 Dose and Shielding

1. *Other than listed below, there are no STAD-canister-specific requirements, or elaborations on dose rate or shielding requirements, beyond those necessary to meet storage and transportation requirements in 10 CFR Parts 72 and 71, respectively, including applicable Acceptance Criteria in associated Review Plans (NUREG-1536 Rev 1, NUREG-1567, and NUREG-1617), with applicable NRC ISG documents.*
2. *The STAD canister shall be designed such that contamination on an accessible external surface shall be removable to*
   a) *1,000 dpm/100 cm^2 – beta-gamma, with a wipe efficiency of 0.1.*
   b) *20 dpm/100 cm^2 – alpha, with a wipe efficiency of 0.1.*

3.1.5 Criticality

1. *Other than listed below, there are no STAD-canister-specific requirements, or elaborations on subcriticality requirements, beyond those necessary to meet storage and transportation requirements in 10 CFR Parts 72 and 71, respectively, including applicable Acceptance Criteria in associated Review Plans (NUREG-1536 Rev 1, NUREG-1567, and NUREG-1617), with applicable NRC ISG documents.*
2. *SFST-ISG-8 Rev 3, Burnup Credit in the Criticality Safety Analyses of PWR Spent Fuel in Transport and Storage Casks, shall be applied.*
3. *SFST-ISG-19, Moderator Exclusion under Hypothetical Accident Conditions and Demonstrating Subcriticality of Spent Fuel under the Requirements of 10 CFR 71.55(e), shall be applied to ensure that moderator exclusion under HAC can be used as a design approach and licensing basis.*
4. *To meet repository objectives, the following four requirements, as a group, are prescribed:*
   a) *Neutron absorber plates or tubes shall be made from borated stainless steel produced by powder metallurgy and meeting ASTM A887-89 (2014), Standard Specification for Borated Stainless Steel Plate, Sheet, and Strip for Nuclear Application, Grade "A" alloys.*

b) Minimum thickness of neutron absorber plates between SNF assemblies shall be 11 mm, assuming single plates. Use of multiple plates between the SNF assemblies (i.e., flux traps) is prohibited.

c) The neutron absorber plate shall have boron content of 1.1 wt % to 1.2 wt %, a range that falls within the specification range for 304B4 (UNS S30464) as described in ASTM A887-89 (2014).

d) Neutron-absorbing material shall extend the full length of the active fuel region, inclusive of any axial shifting within the STAD canister.

Rationale: Borated stainless steel with 1.1-1.2 wt.% of natural boron and a thickness of at least 6 mm has the necessary neutron absorption capacity to maintain subcriticality, while also offering improved durability and corrosion resistance, compared to the aluminum-based neutron absorber materials. In case of an early breach of both the overpack and stainless steel canister, the corrosion of borated stainless steel components is expected. The influx of water vapor or liquid water will promote corrosion of the borated steel under both oxic and anoxic conditions. Use of 304B4 plates that are initially 11 mm thick provides a corrosion allowance of 5 mm. A literature review of the available experimental data on the modes and rates of corrosion for borated stainless steel and their comparison to corrosion of un-borated stainless steel is presented in Appendix A. On the basis of that review, borated stainless steel corrodes more rapidly that non-borated stainless steel. A corrosion rate of 250 nm/year is assumed for borated stainless steel. This value falls within the available rate values for the simulated in-package conditions, and is higher than the borated stainless steel corrosion rates measured in non-aggressive aqueous media. A corrosion rate of 250 nm/yr corresponds to a loss in plate thickness, assuming two-sided corrosion, of 5 mm in 10,000 years. Measured corrosion rates increase with salinity—in seawater, the rates are on the order of 2-11 µm/year. Therefore, special considerations must be made when designing a disposal overpack and internals for a repository where saline groundwater may enter the package. Immediate failure of both overpack and stainless steel canister following permanent disposal is not likely; and therefore the time period during which borated stainless steel components would corrode under either inundated or humid conditions is expected to be shorter than 10,000 years.

If borated stainless steel components are joined using fusion or other hot welding techniques, the welds must be mitigated. Preliminary studies have shown that high temperature annealing at1200 ºC may be sufficient for mitigating damage within the heat-affected zones. Protocols need to be developed for the appropriate weld mitigation. A summary of the welding-induced alterations in borated stainless steel and proposed mitigation techniques is presented in Appendix B.

Borated stainless steel has had limited use as a neutron absorber in dry storage canisters and casks (Greene et al., 2013). Current and proposed storage-related uses of borated stainless steel are discussed in Appendix C. To summarize, two licensed canister designs, the FuelSolutions™ W74 and Transnuclear NUHOMS 52-B (a total of 34 canisters), use borated 304 SS plates as neutron absorber plates. Three dry storage or dual-purpose casks for uncanistered fuel have been designed to use borated stainless steel as a neutron absorber, but only the Castor V/21 is in commercial use, with 25 casks at the Surry Power Station. Borated stainless steel was the design neutron absorber in the Yucca Mountain transportation aging and disposal (TAD) canister (DOE, 2008a), and was accepted by the NRC in their

evaluation of the Yucca Mountain License Application (NRC, 2014b); however, TAD canisters have never been put into use.

A CASTOR V/21 cask at Idaho National Laboratory was opened in 1999, 14 years after loading (NRC, 2001), allowing evaluation of the performance of borated 304 stainless steel within a dry storage cask. The CASTOR V/21 basket is welded 304 stainless steel with integral borated 304 stainless steel plates, and the inspection discovered that weld zones between 304SS and borated 304SS were foci for cracking, which apparently occurred during thermal testing prior to loading, but was not recognized at the time. This is consistent with experimental work showing that welding causes reduced ductility in borated 304 SS (Robino and Cieslak, 1997). As discussed in Appendix B, this effect can be mitigated by post-weld heat treatments.

Limited experimental data is available on the corrosion of borated stainless steel; therefore we have outlined the critical areas for future research. In particular, the modes and rates of corrosion of both borated and un-borated stainless steel under anoxic conditions are not well constrained. Additional experimental work is recommended, and priorities for additional material testing for borated stainless steel are given in Appendix D.

Finally, given the uncertainty associated with corrosion rates for borated stainless steel (Appendix A), there is a possibility that the absorber plates would be significantly degraded, and fail to perform their neutron absorbing function, after fewer than 10,000 years exposure to ground water. Such failure would require breach of the disposal overpack (i.e., from manufacturing defects, corrosion, or disruptive events) before 10,000 years transpires. Moreover, for failure to result in criticality, groundwater chloride concentrations would have to be less than approximately 2 molal; at this concentration or greater, chloride is an effective neutron absorber and criticality is much less likely to occur. Calculating the aggregate probability of these conditions occurring in a repository could be done on a site-specific basis. However, STAD canisters may be implemented before a repository is sited and the disposal environment is known. Hence, a generic (non-site specific) case for postclosure criticality control may be used to improve confidence in STAD canister disposability. The outline of such a case is described in Appendix F.

3.1.6 Confinement and Containment

1. *Other than listed below, there are no STAD-canister-specific requirements, or elaborations on confinement and containment requirements, beyond those necessary to meet storage and transportation requirements in 10 CFR Parts 72 and 71, respectively, including applicable Acceptance Criteria in associated Review Plans (NUREG-1536 Rev 1, NUREG-1567, and NUREG-1617), with applicable NRC ISG documents.*
2. *The STAD canister shall constitute the confinement boundary during storage.*
3. *Helium shall be the STAD canister fill gas for storage and transportation.*
4. *The STAD canister shell and lid shall be designed and fabricated in accordance with ASME (2013) Boiler and Pressure Vessel Code, Section III, Division 1, Subsection NB or NC (for Class 1 Components), to the extent practicable. The vendor shall identify applicable code exceptions, clarifications, interpretations, and code cases.*

3.1.7 Operations

1. *Other than listed below, there are no STAD-canister-specific requirements, or elaborations on operations requirements, beyond those necessary to meet storage and transportation requirements in 10 CFR Parts 72 and 71, respectively, including applicable Acceptance Criteria in associated Review Plans (NUREG-1536 Rev 1, NUREG-1567, and NUREG-1617), with applicable NRC ISG documents.*
2. *The STAD canister lid shall be designed for handling underwater, with the STAD canister in a vertical orientation.*
3. *The STAD canister body and lid shall have features to center and seat the lid during submerged installation.*
4. *A feature for lifting a vertically oriented, loaded STAD canister, with the lifting feature mating with the lid shall be provided. The lifting feature may be integral with the lid or mechanically attached.*
5. *An open, empty, and vertically oriented STAD canister shall have integral lifting feature(s) provided to allow lifting by an overhead handling system.*
6. *It is acceptable to use a carrier approach to load, close, and move STAD canisters in groups to be placed in a storage overpack.*

3.1.8 Materials

1. *Other than listed below, there are no STAD-canister-specific requirements, or elaborations on materials requirements, beyond those necessary to meet storage and transportation requirements in 10 CFR Parts 72 and 71, respectively, including applicable Acceptance Criteria in associated Review Plans (NUREG-1536 Rev 1, NUREG-1567, and NUREG-1617), with applicable NRC ISG documents.*
2. *Required Materials – The STAD canister and structural internals (i.e., basket, but not thermal shunts and criticality control materials) shall be Type 300-series stainless steel as listed in ASTM A-276-13a, Standard Specification for Stainless Steel Bars and Shapes.*
3. *Potential problems from uniform corrosion, pitting, stress corrosion cracking, or other types of corrosion shall be evaluated for the environmental conditions and dynamic loading effects that are specific to the component. Because it is assumed that a disposal overpack will be used for disposal and separately evaluated, this requirement refers to environmental conditions during storage or aging, and during transport.*
4. *All external welds except the closure welds shall be stress relieved prior to loading. The final closure weld shall be capable of being stress relieved after loading.*

Rationale: Items 2, 3, and 4 address the need to consider the potential for canister failure by corrosion during storage. Stainless steels of the 300 series offer many benefits as a canister shell material, including strength, ductility, and weldability. Moreover, they are corrosion-resistant enough that failure by general corrosion within the 150 year design lifetime of the canister is not possible. Failure by pitting or crevice corrosion is also unlikely to occur. However, recent analyses by the Nuclear Waste Technical Review Board (NWTRB, 2010), the Electric Power Research Institute (EPRI, 2011), the DOE Used Fuel Disposition Program (Hanson et al., 2012), and the Nuclear Regulatory Commission (NRC, 2012) have identified the potential for canister penetration by stress corrosion cracking (SCC) as a major concern with respect to the safety performance of long-term interim storage.

The current understanding of canister SCC is discussed in Appendix E. Three criteria must be met for SCC to occur: the metal must be susceptible to SCC; a corrosive (e.g., chloride-

rich) environment must be present; and tensile stresses exceeding a threshold value must be present in the metal. Stainless steels of the 300 series are susceptible to SCC. Moreover, a chloride-rich environment can form on canisters by deliquescence of salt aerosols, which are deposited on the canisters from the air flowing through the storage overpack. Recent canister surface inspections (Bryan and Enos, 2014; EPRI, 2014) have confirmed that chloride salts are present on the surface of in-service SNF storage canisters in near-marine settings; canisters at inland sites have not been evaluated. Finally, residual stress modeling by the NRC has indicated that high tensile stresses are likely to be present in weld and weld heat-affected-zones (HAZ) of canisters currently in service (NRC, 2013). A literature search of measured SCC growth rates indicates that should SCC initiate, penetration of a dry storage canister wall within 150 years is entirely possible (Appendix E). Specification 4 requires post-weld stress mitigation of all canister external welds. This eliminates high tensile stresses present as weld residual stresses, and greatly reduced the risk of canister penetration by SCC.

5. *All metal surfaces shall meet the Surface Cleanliness Classification C requirement defined in ASME NQA-1-2012, Quality Assurance Requirements for Nuclear Facility Applications, Subpart 2.1, Quality Assurance Requirements for Cleaning of Fluid Systems and Associated Components for Nuclear Power Plants.*
6. *The STAD canister and its basket materials shall be designed to be compatible with both borated and unborated pool water.*
7. *The following is a list of prohibited or restricted materials.*
   a) *The STAD canister shall not use organic, hydrocarbon-based, materials of construction.*
   b) *The STAD canister shall not be constructed of pyrophoric materials.*
   c) *The STAD canister (including the basket, thermal shunts, criticality control materials, gaskets, seals, adhesives, and solder) shall not be constructed with materials that would be regulated as hazardous wastes under the Resource Conservation and Recovery Act (RCRA) and prohibited from land disposal under RCRA if declared to be waste. Specific sections of the EPA regulations defining hazardous wastes are listed Section 4 of this document (Glossary).*
8. *The following is a list of marking requirements.*
   a) *The STAD canister shall be capable of being marked on the lid and body with an identical unique identifier prior to delivery for loading.*
   b) *The markings shall remain legible for the service life of the STAD canister of 150 years, without intervention or maintenance during normal operations and off-normal conditions associated with loading, closure, storage, transportation, aging, and placement in a disposal overpack.*

3.1.9 Security

1. *There are no STAD-canister-specific requirements, or elaborations on security requirements, beyond those necessary to meet storage and transportation requirements in 10 CFR Parts 72 and 71, respectively, including applicable Acceptance Criteria in associated Review Plans (NUREG-1536 Rev 1, NUREG-1567, and NUREG-1617), with applicable NRC ISG documents. Note that 10 CFR Parts 72 and 71 invoke compliance with 10 CFR Part 73, Physical Protection of Plants and Materials.*

4. REFERENCES

Albores-Silva, O., Charles, E. and Padovani, C. (2011). Effect of chloride deposition on stress corrosion cracking of 316L stainless steel used for intermediate level radioactive waste containers. *Corrosion Engineering, Science and Technology* **46**, 124-128.

ASTM. (2014). Standard Specification for Borated Stainless Steel Plate, Sheet, and Strip for Nuclear Application. ASTM International.

Beavers, J. A. and Durr, C. L. (1991). *Immersion Studies on Candidate Container Alloys for the Tuff Repository*, NUREG/CR--5598. U.S. Nuclear Regulatory Commission.

Blondes, M. S., Gans, K. D., Thordsen, J. J., Reidy, M. E., Thomas, B., Engle, M. A., Kharaka, Y. K. and Rowan, E. L. (2014). *U.S. Geological Survey National Produced Waters Geochemical Database v2.0 (Provisional)*. U.S.G.S.

Bryan, C. R. and Enos, D. (2014). *Analysis of Dust Samples Collected from Spent Nuclear Fuel Interim Storage Containers at Hope Creek, Delaware, and Diablo Canyon, California*, SAND2014-16383. Albuquerque, NM. Sandia National Laboratories.

Bryan, C. R., Enos, D. G., Brown, N., Brush, L., Miller, A. and Norman, K. (2011). *Engineered Materials Performance: Gap Analysis and Status of Existing Work*, FCRD-USED-2011-000407. U.S. Department of Energy.

BSC. (2004). *Aqueous Corrosion Rates for Waste Package Materials*. Las Vegas, NV. Office of Civilian Radioactive Waste Management, U.S. Department of Energy.

BSC. (2008). *Multiscale Thermohydrologic Model*, ANL-EBS-MD-000049 Rev. 3. Las Vegas, NV. Office of Civilian Radioactive Waste Management, U.S. Department of Energy.

Chen, Z. and Kelly, R. (2010). Computational modeling of bounding conditions for pit size on stainless steel in atmospheric environments. *Journal of the Electrochemical Society* **157**, C69-C78.

Cook, A., Lyon, S., Stevens, N., Gunther, M., McFiggans, G., Newman, R. and Engelberg, D. (2014). Assesing the Risk of Under-Deposit Chloride-Induced Stress Corrosion Cracking in Austenitic Stainless Steel Nuclear Waste Containers. *Corrosion Engineering, Science and Technology* **49**, 529-534.

Cook, A., Stevens, N., Duff, J., Mishelia, A., Leung, T. S., Lyon, S., Marrow, J., Ganther, W. and Cole, I. (2011). Atmospheric-induced stress corrosion cracking of austenitic stainless steels under limited chloride supply. *Proc. 18th Int. Corros. Cong., Perth, Australia.*

DOE. (1996). *Title 40 CFR Part 191 compliance certification application for the Waste Isolation Pilot Plant, Vol. 1-21*, DOE/CAO-1994-2184. Carlsbad, NM. Carlsbad Area Office, U.S. Department of Energy.

DOE. (2008a). *Transportation, Aging and Disposal Canister System Performance Specification*, DOE/RW-0585 WMO-TADCS-000001 Rev1/ICN1. U.S. Department of Energy, Office of Civilian Radioactive Waste Management.

DOE. (2008b). *Yucca Mountain Repository License Application*, DOE/RW-0573, Rev. 1. Washington, D.C. Office of Civilian Radioactive Waste Management, U.S. Department of Energy.

Elboujdaini, M. (2011). Hydrogen-Induced Cracking and Sulfide Stress Cracking. In: Revie, R. W. (ed.) *Uhlig's Corrosion Handbook*. John Wiley & Sons, Inc.

EnergySolutions Spent Fuel Division Inc. (2007). *FuelSolutions™ W74 Canister Storage Final Safety Analysis Report Revision 6*. Campbell, CA.

EPRI. (1994). *Borated Stainless Steel Joining Technology. Final Report.*, TR-104627. Palo Alto, CA. EPRI.

EPRI. (2005). *Handbook on Neutron Absorber Materials for Spent Nuclear Fuel Applications*. Palo Alto, CA. Electric Power Research Institute.

EPRI. (2011). *Extended Storage Collaboration Program (ESCP) Progress Report and Review of Gap Analyses*. Palo Alto, CA.

EPRI. (2014). *Calvert Cliffs Stainless Steel Dry Storage Canister Inspection*. Palo Alto, CA.

Fairweather, N., Platts, N. and Tice, D. (2008). Stress-Corrosion Crack Initiation Of Type 304 Stainless Steel In Atmospheric Environments Containing Chloride: Influence Of Surface Condition Relative Humidity Temperature And Thermal Sensitization. *CORROSION 2008*.

Fix, D. V., Estill, J. C., Wong, L. L. and Rebak, R. B. (2004). *General and localized corrosion of austenitic and borated stainless steels in simulated concentrated ground waters*. San Diego, CA. ASME-Pressure Vessels and Piping.

Frape, S., Blyth, A., Blomqvist, R., McNutt, R. and Gascoyne, M. (2003). Deep Fluids in the Continents: II. Crystalline Rocks. In: Holland, H. & Turkenian, K. (eds.) *Treatise on Geochemistry*. ElSevier, 541-580.

Freeze, G., Voegele, M., Vaughn, P., Prouty, J., Nutt, W. M., Hardin, E. and Sevougian, S. D. (2013). *Generic Deep Geologic Disposal Safety Case*, FCRD-UFD-2012-000146 Rev. 1. U.S. Department of Energy, Office of Used Nuclear Fuel Disposition.

García, C., Martín, F., De Tiedra, P., Heredero, J. and Aparicio, M. (2001). Effects of prior cold work and sensitization heat treatment on chloride stress corrosion cracking in type 304 stainless steels. *Corrosion Science* **43**, 1519-1539.

Greene, S. R., J.S., M. and Macy, S. A. (2013). *Storage and Transport Cask Data For Used Commercial Nuclear Fuel: 2013 U.S. Edition*. Oak Ridge, TN. EnergX, LLC/Advanced Technology Insights, LLC.

Hanson, B., Alsaed, H., Stockman, C., Enos, D., Meyer, R. and Sorenson, K. (2012). *Gap analysis to support extended storage of used nuclear fuel*, FCRD-USED-2011-000136. U.S. Department of Energy.

Hardin, E. (2013). *Temperature-Package Power Correlations for Open-Mode Geologic Disposal Concepts*, SAND2014-1425. Albuquerque, NM. Sandia National Laboratories.

Hardin, E., Bryan, C., Ilgen, A., Kalinina, E., Banerjee, K., Clarity, J., Howard, R., Jubin, R., Scaglione, J., Perry, F., Zheng, L., Rutqvist, J., Birkholzer, J., Greenberg, H., Carter, J. and Severynse, T. (2014). *Investigations of Dual-Purpose Canister Direct Disposal Feasibility (FY14)*, FCRD-UFD-2014-000069 Rev. 0. U.S. Department of Energy, Office of Used Nuclear Fuel Disposition.

Hardin, E., Clayton, D. J., Martinez, M. J., Neider-Westerman, G., Howard, R. L., Greenberg, H. R., Blink, J. A. and Buscheck, T. A. (2013). *Collaborative Report on Disposal Concepts*, FCRD-UFD-2013-000170. U.S. Department of Energy, Office of Used Nuclear Fuel Disposition.

Hardin, E., Hadgu, T., Clayton, D., Howard, R., Greenberg, H., Blink, J., Sharma, M., Sutton, M., Carter, J., Dupont, M. and Rodwell, P. (2012). *Repository Reference Disposal Concepts and Thermal Management Analysis*, FCRD-USED-2012-000219 Rev. 2. U.S. Department of Energy, Office of Used Nuclear Fuel Disposition.

Hardin, E. and Howard, R. (2013). *Assumptions for Evaluating Feasibility of Direct Geologic Disposal of Existing Dual-Purpose Canisters*, FCRD-UFD-2012-000352 Rev.01. U.S. Department of Energy, Office of Used Nuclear Fuel Disposition.

Hardin, E. and Kalinina, E. (2015). *Cost Estimation Inputs for Spent Nuclear Fuel Geologic Disposal Concepts*, SAND2015-0687. Albuquerque, NM. Sandia National Laboratories.

Hayashibara, H., Mayuzumi, M. and Mizutani, Y. (2008). Effects of temperature and humidity on atmospheric stress corrosion cracking of 304 stainless steel. *CORROSION 2008*.

He, X. (2008). Corrosion performance of neutron-absorbing borated stainless steel. 24 June, 2008. *Presented to ASTM C26 – nuclear fuel cycle C260300 subcommittee on neutron absorber materials*.

He, X., Ahn, T. and Sippel, T. (2012). Corrosion of Borated Stainless Steel In Water And Humid Air. *CORROSION 2012*: Citeseer.

Ilgen, A., Enos, D., Bryan, C., Rechard, R. and Hardin, E. (2014). *Experimental Plan for DPC/Overpack Performance in a Repository*, FCRD-UFD-2014-000596. U.S. Department of Energy, Office of Used Nuclear Fuel Disposition.

Jack, T. R. and Wilmott, M. J. (2011). Corrosion by soils. In: Revie, R. W. (ed.) *Uhlig's Corrosion Handbook*. John Wiley & Sons, Inc.

Kain, R. M. (1990). Marine atmosphere corrosion cracking of austenic stainless steels. *Materials Performance* **29**, 60-62.

Khatak, H., Gnanamoorthy, J. and Rodriguez, P. (1996). Studies on the influence of metallurgical variables on the stress corrosion behavior of AISI 304 stainless steel in sodium chloride solution using the fracture mechanics approach. *Metallurgical and Materials Transactions A* **27**, 1313-1325.

Kondo, Y. (1989). Prediction of fatigue crack initiation life based on pit growth. *Corrosion* **45**, 7-11.

Kosaki, A. (2008). Evaluation method of corrosion lifetime of conventional stainless steel canister under oceanic air environment. *Nuclear Engineering and Design* **238**, 1233-1240.

Krouse, D., Laycock, N. and Padovani, C. (2014). Modelling pitting corrosion of stainless steel in atmospheric exposures to chloride containing environments. *Corrosion Engineering, Science and Technology* **49**, 521-528.

Kursten, B., Smailos, E., Azkarate, I., Werme, L., Smart, N. R. and Santarini, G. (2004). *COBECOMA: State-of-the-art document on the COrrosion BEhaviour of COntainer MAterials. European Commission 5th Euratom Framework Programme, 1998-2002*, Contract no. FIKW-CT-20014-20138 Final Report. European Commission.

Lister, T. E., Mizia, R. E., Ericksen, A. and Birk, S. M. (2007). *Electrochemical corrosion testing of borated stainless steel alloys*, EXT-07-12633. INL.

Lister, T. E., Mizia, R. E., Erickson, A. W. and Matteson, B. S. (2008). General and localized corrosion of borated stainless steel. *Corrosion*: NACE.

Martin, J. (1989). Effects of processing and microstructure on the mechanical properties of boron-containing austenitic stainless steels. *Waste processing, transportation, storage and disposal, technical programs and public education*.

McCright, R. D., W.G., H. and Van Konynenburg, R. A. (1987). *Progress Report on the Results of Testing Advanced Conceptual Design Metal Barrier Materials under Relevant Environmental Conditions for a Tuff Repository*, UCID-21044. Lawrence Livermore Naitonal Laboratory.

Mintz, T. S., Caseres, L., He, X., Dante, J., Oberson, G., Dunn, D. S. and Ahn, T. (2012). Atmospheric Salt Fog Testing to Evaluate Chloride-Induced Stress Corrosion Cracking of Type 304 Stainless Steel. *Corrosion 2012*. Salt Lake City, March 11-15: NACE.

Moreno, D., Molina, B., Ranninger, C., Montero, F. and Izquierdo, J. (2004). Microstructural Characterization and Pitting Corrosion Behavior of UNS S30466 Borated Stainless Steel. *Corrosion* **60**, 573-583.

Nakayama, G. (2006). Atmospheric stress corrosion cracking (ASCC) susceptibility of stainless alloys for metallic containers. In: VanIseghem, P. (ed.) *Scientific Basis for Nuclear Waste Management XXIX*, pp. 845-852.

Nakayama, G. and Sakakibara, Y. (2013). Prediction Model for Atmospheric Stress Corrosion Cracking of Stainless Steel. *ECS Transactions* **50**, 303-311.

NDA. (2012). *Industry Guidance - Interim Storage of Higher Activity Waste Packages – Integrated Approach*. West Cumbria, UK. Nuclear Decommissioning Authority.

NRC. (1993). *Certificate of Compliance for Dry Spent Fuel Storage Casks: TN-24 Dry Storage Cask*, ID# 72-1005, ADAMS ML033020128. Washington D.C. U.S. Nuclear Regulatory Commission.

NRC. (2001). *Dry Cask Storage Characterization Project-Phase 1: CASTOR V/21 Cask Opening and Examination*, NUREG/CR-6745. Washington D.C. U.S. Nuclear Regulatory Commission.

NRC. (2012). *Identification and Prioritization of the Technical Information Needs Affecting Potential Regulation of Extended Storage and Transportation of Spent Nuclear Fuel. Draft for comment.* Washington, D.C. U.S. NRC.

NRC. (2013). *Finite Element Analysis of Weld Residual Stresses in Austenitic Stainless Steel Dry Cask Storage System Canisters*, NRC Technical Letter Report (ADAMS ML13330A512). Washington D.C. Nuclear Regulatory Commission.

NRC. (2014a). *Assessment of Stress Corrosion Cracking Susceptibility for Austenitic Stainless Steels Exposed to Atmospheric Chloride and Non-Chloride Salts*, NUREG/CR-7170. Washington D.C. U.S. Nuclear Regulatory Commission.

NRC. (2014b). *Safety Evaluation Report Related to Disposal of High-Level Radioactive Wastes in a Geologic Repository at Yucca Mountain, Nevada. Vol. 3: Repository Safety After Permanent Closure*, NUREG-1949. Washington, D.C. U.S. Nuclear Regulatory Commission.

NWTRB. (2010). *Evaluation of the Technical Basis for Extended Dry Storage and Transportation of Used Nuclear Fuel*. NWTRB.

Park, T.-D., Baek, K.-K. and Kim, D.-S. (1997). PWHT effect on the mechanical properties of borated stainless steel GTA weldments for nuclear shield. *Metals and Materials* **3**, 46-50.

Parrott, R. and Pitts, H. (2011). *Chloride stress corrosion cracking in austenitic stainless steel: Assessing susceptibility and structural integrity.* U.K. Health and Safety Executive.

Prosek, T., Iversen, A. and Taxén, C. (2009). Low temperature stress corrosion cracking of stainless steels in the atmosphere in presence of chloride deposits. *Corrosion* **65**, 105-117.

Prosek, T., Le Gac, A., Thierry, D., Le Manchet, S., Lojewski, C., Fanica, A., Johansson, E., Canderyd, C., Dupoiron, F. and Snauwaert, T. (2014). Low temperature stress corrosion cracking of austenitic and duplex stainless steels under chloride deposits. *Corrosion*.

Rebak, R. B. (2011). Environmental Degradation of Engineered Barrier Materials in Nuclear Waste Repositories. In: Revie, R. W. (ed.) *Uhlig's Corrosion Handbook*. John Wiley & Sons, Inc.

Robino, C. and Cieslak, M. (1995). High-temperature metallurgy of advanced borated stainless steels. *Metallurgical and Materials Transactions A* **26**, 1673-1685.

Robino, C. and Cieslak, M. (1997). Fusion welding of a modern borated stainless steel. *Welding Journal-Including Welding Research Supplement* **76**, 11-11.

Shirai, K., Tani, J., Arai, T., Wataru, M., Takeda, H. and Saegusa, T. (2011). SCC evaluation test of a multi-purpose canister. 10-14 April. *13th International High-Level Radioactive Waste Management Conference (IHLRWMC)*. Albuquerque, NM: American Nuclear Society, 824-831.

SKB. (2011). *Long-term safety for the final repository for spent nuclear fuel at Forsmark: Main report of the SR-Site project. 3 Volumes*, SKB TR-11-01. Stockholm. Svensk Karnbranslehantering AB.

SNL. (2007a). *Analysis of Mechanisms for Early Waste Package / Drip Shield Failure*, ANL-EBS-MD-000076 Rev. 0. Las Vegas, NV. Sandia National Laboratories.

SNL. (2007b). *Geochemistry Model Validation Report: Material Degradation and Release Model* Las Vegas, NV. Sandia National Laboratories.

Sridhar, N., Wilde, B., Manfredi, C., Kesavan, S. and Miller, C. (1991). *Hydrogen Absorption and Embrittlement of Candidate Container Materials*, CNWRA 91-008. CNWRA.

Streicher, M. A. and Grubb, J. F. (2011). Austenitic and ferritic stainless steels. In: Revie, R. W. (ed.) *Uhlig's Corrosion Handbook*. John Wiley & Sons, Inc.

Tani, J. I., Mayuzurmi, M. and Hara, N. (2009). Initiation and propagation of stress corrosion cracking of stainless steel canister for concrete cask storage of spent nuclear fuel. *Corrosion* **65**, 187-194.

Taylor, M. F. (1994). The Significance of Salt Contamination on Steel Surfaces, Its Measurement and Removal. *UK Corrosion and Eurocorr 94 : 31 October-3 November 1994,* . Bournemouth International Centre, UK.

Tokiwai, M., Kimura, H. and Kusanagi, H. (1985). The amount of chlorine contamination for prevention of stress corrosion cracking in sensitized type 304 stainless steel. *Corrosion Science* **25**, 837-844.

Turnbull, A., McCartney, L. and Zhou, S. (2006a). A model to predict the evolution of pitting corrosion and the pit-to-crack transition incorporating statistically distributed input parameters. *Corrosion Science* **48**, 2084-2105.

Turnbull, A., McCartney, L. and Zhou, S. (2006b). Modelling of the evolution of stress corrosion cracks from corrosion pits. *Scripta materialia* **54**, 575-578.

Turnbull, A. and Zhou, S. (2004). Pit to crack transition in stress corrosion cracking of a steam turbine disc steel. *Corrosion Science* **46**, 1239-1264.

Upadhyay, N., Pujar, M., Das, C., Mallika, C. and Mudali, U. K. (2014). Pitting Corrosion Studies on Solution-Annealed Borated Type 304L Stainless Steel Using Electrochemical Noise Technique. *Corrosion* **70**, 781-795.

Woldemedhin, M. T. and Kelly, R. G. (2014). Evaluation of the maximum pit size model on stainless steel under atmospheric conditions. *ECS Transactions* **58**, 41-50.

Wu, G. and Modarres, M. (2012). A Probabilistic-Mechanistic Approach to Modeling Stress Corrosion Cracking in Alloy 600 Components with Applications. Presentation, PSAM 2011

Appendix A

Borated vs. Non-Borated Stainless Steel: Corrosion Rates and Mechanisms

Borated stainless steel is proposed for the construction of the absorber plates (or, other neutron absorber configurations) to be placed in the transportation, aging, and disposal canister. Due to the low solubility of boron in stainless steel, maximum boron content of these alloys is limited to 2.25 wt.% (EPRI, 2005). If natural boron is used, the required thickness of plates is relatively large: to achieve an areal density of 0.030 gm B-10/cm^2, a plate thickness of 12.5 mm (0.5 inch) at a boron loading of 1.7 wt.% is required (EPRI, 2005). ASTM-A887-89 includes the definition for the two boron stainless steel absorbers which are available and have been used as neutron absorber materials (ASTM, 2014). Here we review available experimental results on the modes and rates of corrosion for the borated stainless steels and compare to the representative rates measured for the non-borated analogs under conditions representative of geologic storage.

Applicable environmental conditions

Environmental factors, such as aqueous chemistry, redox potential and microbial activity strongly influence the corrosion rates of stainless steel alloys. In particular, the corrosion mechanism, rate, and corrosion products are controlled by the availability of dissolved oxygen. As a rule, general and localized corrosion proceed faster in oxic conditions, where cathodic reactions on metallic surfaces are dominated by the reduction of dissolved oxygen (Rebak, 2011). Most geologic repository types are expected to return to anoxic or anaerobic conditions shortly after backfilling and closure, particularly, repositories in a low-permeability, water saturated host media that contain reducing minerals (e.g., pyrite) or natural organic matter (Bryan et al., 2011). In the absence of oxygen, water acts as an electron acceptor for metallic iron, and the cathodic reaction is controlled by hydrogen evolution (Rebak, 2011). The ubiquity of water as a possible electron acceptor is one reason that steels continue to corrode under anoxic aqueous conditions. While steel corrosion is generally anticipated to be slower under anoxic conditions, environmental factors such as sulfide concentration or microbial activity may result in rapid corrosion even under anoxic conditions (Jack and Wilmott, 2011).

Corrosion rates of stainless steels 304/304L and 316/316L under oxic conditions

Uniform Corrosion – Uniform corrosion of stainless steel under oxic, alkaline conditions, and the water chemistry typical of a clay repository (no added chloride) vary from <0.1 μm yr^{-1} at 30 ºC to 0.2-0.8 μm yr^{-1} at 80 ºC (Kursten et al., 2004). Beavers and Durr (1991) performed immersion tests on the artificially creviced samples of 304L in fresh water, J-13, simulated J-13, J-13 with crushed tuff water, and simulated concentrated waters at 90 °C with the resulting corrosion rate of <0.2 μm yr^{-1}. Driven corrosion tests in aerated simulated J-13 well water at 90 °C gave a corrosion rate of 0.02-0.14 μm yr^{-1} in liquid, and 0.96-2.95 μm yr^{-1} in vapor. Beavers and Durr (1991) tested the effect of added hydrogen peroxide (electrolysis product) on 304L and measured rates of 0.04-6.58 μm yr^{-1}. The corrosion rates of the 304 L reported by McCright et al. (1987) after a yearlong exposure to J-13 tuff water, performed under both irradiated and non-irradiated conditions at room temperature are 0.151 μm yr^{-1} (irradiated) and 0.285 μm yr^{-1} (non-irradiated).

Localized Corrosion – The presence of chloride poses one of the strongest chemical controls on whether pitting will take place. Experimental testing indicated no pitting of 316L in alkaline solutions containing up to 100 g L^{-1} chloride at room temperature of 21 ºC (Kursten et al., 2004). When the concentration of chloride is 50 g L^{-1}, a critical pitting temperature of 45 ºC was reported (Kursten et al., 2004). Similar chloride concentration threshold behavior was observed for pitting of 304L: pitting was observed at 60 ºC

with >50 g L^{-1} chloride (Kursten et al., 2004). Crevice corrosion of 304L was observed at 80 ºC and background chloride concentrations of 20 g L^{-1} or greater; and no crevice corrosion was observed at 40 ºC and chloride concentrations up to 20 g L^{-1} (Kursten et al., 2004). Pit initiation testing for 304/304L and 316/316L indicates that pitting progression varies: in particular, the oxidative history of the sample is associated with a large difference in the number of pits for the 316/316L alloys, but not for 304/304L. Beavers and Durr (1991) show that in a relatively aggressive aqueous media at 90 °C, creviced samples have corrosion rates of 0.03 μm yr^{-1} in vapor, and 0.29-0.43 μm yr^{-1} in liquid with significant pitting with pit depths of 15-62 μm after 2855 hours of testing.

Stress corrosion cracking is observed in an unstressed sample of 304L stainless steel after aging in cementitious material containing 100 g L^{-1} chloride for 2 years (Kursten et al., 2004). Additional testing in alkaline solutions indicated that increased chloride (17.7 g L^{-1}) and thiosulfate ($S_2O_3^{2-}$ at 3.4 g L^{-1}) increased both pitting and stress corrosion cracking of the 316L and 304L alloys (Kursten et al., 2004). In aggressive environments (e.g., 45% MgCl or 26% NaCl), stress corrosion cracking is observed to take place within hours to days. Cracking is observed in less than 3 hours in magnesium chloride solution at 155°C, and after 48 to 72 hours in sodium chloride tests at 102 and 200°C (Streicher and Grubb, 2011).

Corrosion rates of stainless steels 304/304L and 316/316L under anoxic conditions

Uniform Corrosion – Significantly less experimental data is available on the corrosion of stainless steel under anoxic conditions. Uniform corrosion rates of stainless steel measured under anoxic conditions and the water chemistry typical of a clay repository (no added chloride) are from 0.001 μm yr^{-1} to 0.1 μm yr^{-1} at 30ºC and 80ºC respectively (Kursten et al., 2004).

Localized Corrosion – Localized corrosion under anoxic conditions includes hydrogen embrittlement, sulfide stress cracking (Elboujdaini, 2011), and microbially-assisted corrosion. Hydrogen gas is produced during anoxic corrosion of stainless steel. Hydrogen embrittlement, induced blistering, and cracking may occur due to the evolution of atomic hydrogen at the surface, followed by the diffusion of atomic hydrogen into steel (Elboujdaini, 2011). Sridhar et al. (1991) states, that in a typical repository setting, hydrogen embrittlement is, most likely, minor in comparison to other corrosion modes; however, the rate of hydrogen evolution and diffusion must be determined on a case by case basis. Sulfide stress cracking is a variety of hydrogen-induced cracking, and is usually localized in weld zones (Elboujdaini, 2011). It can occur in mildly corrosive media at temperatures below 90°C. A few studies report that microbially-assisted corrosion may significantly shorten the lifetime of a stainless steel component

Corrosion of borated stainless steel under oxic conditions

Uniform Corrosion – Lister et al. (2007) performed electrochemical corrosion testing of borated stainless steel alloys, and measured the uniform corrosion rate of 17.6 - 37.1 nm yr^{-1} at 60 °C in an aerated simulated in-package solution. The authors state that the results are indicative of the short-term corrosion rates, and that a longer term test would be required for a comprehensive prediction of the borated stainless steel behavior in a waste package.

The uniform corrosion rate of Neutronit (steel alloy with neutron absorbers) is assumed to be similar to the corrosion rate of stainless steel Type 321 (BSC, 2004), which varies as a function of water composition (freshwater vs. saltwater) and temperature. The measured values are 0.001-0.011± 0.004 (1σ) μm yr^{-1} in fresh water at 29.5 °C, 0.025-0.33 ± 0.088 (1σ) μm yr^{-1} in freshwater at 50 °C, and 1.81-11.06 ± 10.19 (1σ) μm yr^{-1} in saltwater at 26.7°C (BSC, 2004).

Localized Corrosion – Fix et al. (2004) measured weight loss in simulated concentrated groundwater at 90°C, where samples were immersed for more than 5 years. The weight loss was mostly caused by the localized corrosion (therefore, general corrosion rates are not calculated). He (2008) reports that in chloride solutions, borated stainless steel is susceptible to localized corrosion and general corrosion rates vary from tens of nm yr^{-1} to μm yr^{-1} depending on the test environment and duration. He et al. (2012) performed tests in water vapor and under immersed (simulated groundwater) conditions for Types 304B4

and 304B5 borated stainless steel at 60, 75, and 90 °C. Pitting corrosion was observed when specimens were exposed to humid air at 75 and 90 °C, and no pitting occurred at temperature of 60 °C (He et al., 2012).

Borated alloy (UNS S30466, same as borated 304) is susceptible to pitting in the presence of sulfide and chloride ions (Moreno et al., 2004). Another electrochemical study also reports pitting corrosion of borated stainless steel (with 1.2% B) in 0.5 M sodium chloride solution. Pitting was decreased with increasing degree of solution-annealing (Upadhyay et al., 2014).

Corrosion of borated stainless steel under anoxic conditions

Similarly to the non-borates stainless steels, there is significantly less data available on the corrosion of borated stainless steel under anoxic conditions. Lister et al. (2008) measured the corrosion rate of three borated stainless steel 304B alloys with varying boron content at 60 °C. Samples were creviced, and potentiostatic tests were performed in anoxic conditions and in an acidic environment. The tests were performed over the course of 7 days under a nitrogen gas purge. The measured corrosion rate increased as a function of the boron content. The average corrosion rates were 221 ± 70 nm yr^{-1} for 304B4 (1.17 % B), 427 ± 132 nm yr^{-1} for 304B5 (1.32 % B), and 464 ± 100 nm yr^{-1} for 304B6 (1.69 % B) (Lister et al., 2008).

Comparison of borated vs. non-borated stainless steel corrosion rates

Fix, et al. (2004), He (2008), SNL (2007b), and NRC (2014b) indicate that the corrosion rates of borated stainless steels are higher than for unborated Types 304 and 316. Fix et al. (2004) measured weight loss in simulated concentrated groundwater at 90°C, where samples were immersed for more than 5 years. The results indicate that borated alloys are less resistant to the general corrosion, as well as to the localized attack. The borated stainless had weight loss 3 to 10 times higher than the non-borated materials, and the weight loss was mostly caused by the localized corrosion. The SNL (2007b) report summarizes linear polar resistance (LPR) analyses on the borated stainless steel Types 304B4 and 304B5 with the average reported corrosion rate of 7.3 – 44.4 nm yr^{-1} (LPR) and 42.3 - 95.6 nm yr^{-1} for gravimetric tests. These rates were measured under relatively non-aggressive conditions (starting pH 5.5 to 7, low ionic strength, 60 °C) and are 3.5 to 5.5 times greater than the rates measured in analogous experiments for the non-borated Type 304L.

A variety of tests summarized in the BSC (2004) report indicate that corrosion of borated Type 304 stainless steel is faster than for the non-borated counterpart. The rate depends on the amount of boron in the alloy (0.3 and 1.5 % alloys were tested), temperature, and aqueous matrix composition. The mean values for the Types 302/304/304L vary from 0.214 μm yr^{-1} for freshwater at up to 100 °C to 11.44 μm yr^{-1} for saltwater at 26.7 °C. The values for the borated stainless steel under similar testing conditions ranged from 6.10 μm yr^{-1} (0.3% B, ambient temperature and freshwater) to 210.31 μm yr^{-1} (1.5% B, ambient-boiling temperature, freshwater) to 453.74 μm yr^{-1} (1.5% B, ambient-boiling temperature, and harsh aqueous matrix).

Summary of literature values for general corrosion rates for stainless steel and borated stainless steel is shown in Table A-1.

Table A-1. Corrosion rates of borated and non-borated stainless steels

Uniform corrosion rates for borated stainless steel					
Min nm/year	**Max nm/year**	**Temp °C**	**Media**	**Oxic/ Anoxic**	**Ref.**
17.6	37.1	60	simulated in-package water	Oxic	Lister et al. (2007)
1	11	29.5	freshwater	Oxic	BSC (2004)
25	33	50	freshwater	Oxic	BSC (2004)
1810	11060	26.7	saltwater	Oxic	BSC (2004)
7.3	95.6	60	non-aggressive	Oxic	SNL (2007b)
221	464	60	simulated in-package water	Anoxic	Lister et al. (2008)
Uniform corrosion rates for non-borated stainless steel					
200	800	30-80	fresh water	Oxic	Kursten et al (2004)
20	140		liquid	Oxic	Beavers and Durr (1991)
960	2950		vapor	Oxic	Beavers and Durr (1991)
40	6580		with hydrogen peroxide	Oxic	Beavers and Durr (1991)
151	285		J-13 water, both irradiated and non-irradiated	Oxic	McCright et al. (1987)
1	100	30-80	fresh water	Anoxic	Kursten et al. (2004)

Appendix B

Welding-Induced Alteration of Borated Stainless Steel and Methods for Weld Mitigation

ASTM-A887-89 describes eight borated stainless steel alloys (Types) with varying boron content (0.20% to 2.35% boron), with two grades specified for each. Grade "A" must have smaller and more spherical boride Cr_2B particles, in comparison to Grade "B", and therefore Grade "A" alloys have better mechanical properties. Only Grade "A" alloys are considered for the STAD canisters. The weldability of borated stainless steel is similar to the traditional austenitic steels (Robino and Cieslak, 1997), and can be achieved using a variety of welding techniques. The welds have diminished ductility, compared to the ductility of the alloy, away from the heat affected zone (Robino and Cieslak, 1997; EPRI, 2005). The loss of ductility is due to aggregation and coalescence of boride particles at the grain boundaries between the molten zone of the filler weld metal (EPRI, 2005). Due to this diminished performance of the welded components, the US Nuclear Regulatory Commission discourages the use of ASTM 887 borated stainless steel as a structural component for spent fuel storage racks (EPRI, 2005).

Fusion welding (e.g. tungsten arc (GTA) and electron beam welding) damage can be mitigated to some degree by the postweld heat treatment. Several studies have shown that the ASME code minimum required impact toughness can be achieved after annealing of the welded zone (EPRI, 1994; Park et al., 1997; Robino and Cieslak, 1997).

Robino and Cieslak (1997), determined that for the fusion welded 304B4 Grade A alloy (1.16 wt.% B) postweld heat treatment requires 28500 hours (at 700 °C), 170 hours (900 °C), 24 hours (1000 °C), and 1.05 hours (at 1200 °C) for the weld damage to be mitigated to near Code-acceptable levels. Park et al., 1997, investigated GTA welds of AlSI 304-B3 stainless steel plates, which were annealed either at 700~1100°C for 1 hour or at 1100°C and 1200°C, for 1~7 hours. A variety of tests (bending tests, elongation tests, and Charpy impact tests) were in agreement that the higher temperature of 1200 °C is necessary to reverse the loss of mechanical properties of the heat affected zones.

These studies indicate that postweld heat treatment at the temperature as high as 1200°C is necessary for the welds to have ductility matching that of base metal. Additional research is needed to optimize the postweld heat treatment procedures.

Appendix C

Review of the Use of Borated Stainless Steel in Existing Designs

This Appendix reviews current uses of borated 304 stainless steel as a neutron absorber in the nuclear industry. Neutron absorber materials that are currently in use consist mostly of aluminum–based materials. These fall into two groups. The first are aluminum alloys or metal matrix composites containing boron as a neutron absorber, usually in the form of a metal boride. The second commonly used type is a ceramic-metal material (cermet), produced by mixing powdered Al and carbon boride together, placing it between sheets of aluminum, and rolling at high temperatures to produce a sandwich containing the sintered Al-metal-carbon boride mixture). Borated stainless steel is more rarely used, and has both advantages and disadvantages relative to Al-based materials. Because possible boron loadings are relatively low (<2.5 wt%), thicker plates borated stainless are required to achieve the required mass loadings per unit area of boron, adding to the volume and weight of the absorber plates. However, borated stainless has a much higher strength and lower corrodibility than Al materials.

Use of borated stainless steel as opposed to and Al-based absorber material is required in the standardized storage and disposal canister for two reasons, both related to postclosure performance of the STAD and internals in a repository environment. Although a protective overpack for the canister is assumed to be present, the neutron absorber materials must be sufficiently corrosion-resistant to remain intact and mitigate criticality concerns for 10,000 years in the case of early failure of the overpack and canister. First, borated stainless steel will not form a galvanic couple with other metals used in the canister internals, as an Al-based neutron absorber would. Galvanic coupling would result in the neutron absorber plate acting as a sacrificial anode, corroding rapidly away. Second, even in the absence of a galvanic reaction, Al corrosion rates are sufficiently high in aqueous systems such as a flooded canister, that the integrity of the neutron absorber materials for 10,000 years could not occur. Borated stainless steel corrosion rates, while more rapid that those of non-borated stainless steel, are much slower than Al corrosion rates (Appendix A). Even borated stainless steel absorber plates may not maintain sufficient thickness to limit criticality if canister overpacks fail immediately upon emplacement. However, while overpacks have not yet been designed, the anticipated overpack performance would prevent borated steel plates from being exposed to aqueous conditions for a minimum of many thousands of years after emplacement.

A list of storage systems using borated 304 SS, as of August 2013, is given in Greene *et al.* (2013). They are listed below.

Canister systems using borated 304SS:

FuelSolutions™ W74M and W74T Canisters – The FuelSolutions™ W74M is a 64 BWR multipurpose canister licensed for storage and transportation and intended for disposal (Greene et al., 2013). The W74T is designed only for storage and transportation. The W74 canisters can also accept up to eight damaged fuel cans. Borated 304SS absorber plates line each cell in the basket, and are held in position by welded stainless steel retainers that insert into holes in the sheets to hold them into position (EnergySolutions Spent Fuel Division Inc., 2007). The neutron absorber plates are non-structural members. Only seven W74 canisters are currently in use, all at the Big Rock Point Nuclear Plant.

Transnuclear NUHOMS 52B Canister – The Transnuclear NUHOMS 52B is a 52 BWR canister licensed for storage only. It has a carbon steel basket with borated 304SS absorber plates. Twenty-seven canisters are currently in use at the Susquehanna Nuclear Power Plant (Greene et al., 2013).

Casks for non-canistered fuel—storage-only and dual-purpose

CASTOR V/21 Cask – The CASTOR V/21 cask is a 24 PWR storage cask for uncanistered SNF. The fuel basket is constructed of welded 304 SS, with integral plates of borated stainless steel for criticality control (Greene et al., 2013). Twenty-five CASTOR V/21 casks are in currently in use at the Surry Nuclear Power Station, and one is at Idaho National Engineering Laboratory.

The cask at INEL was loaded in 1985 and opened in 1999 to assess the effects of long term interim storage on the SNF and cask internals (NRC, 2001). During the 1999 inspection, it was determined that 15 of 16 examined stitch welds—welds that attached the borated 304SS neutron absorber plates to the 304SS basket structure—had cracked. However, these weld locations had not been examined prior to loading in 1985, and it was determined that the cracking probably occurred due to differential thermal expansion during testing prior to cask loading. Other, more accessible basket welds that were examined in 1985 had shown cracking at that time.

The weld cracks illustrate one flaw of borated 304SS; welding decreases the ductility of the material. This change in material performance is attributed to re-dissolution of the borides in the weld zone and formation a dendritic austenite/boride eutectic (Robino and Cieslak, 1995); some researchers (Martin, 1989) have suggested that the eutectic may also form in the heat affected zone and that boride grains will agglomerate there, but that has been disputed (Robino and Cieslak, 1995). The decrease in ductility is greatest at the HAZ-weld fusion line, and it is here that cracking tends to occur. This effect is less important for Grade A borated 304SS than for Grade B, which has larger and less evenly dispersed boride grains than Grade A. Because of the reduced ductility in borated stainless steel weld zones, the US Nuclear Regulatory Commission has objected to the use of ASTM 887 borated stainless steel as a structural component for spent fuel storage racks (EPRI, 2005).

TN-24 Cask – The Transnuclear TN-24 and TN-24P storage casks were designed for the storage and transportation of spent nuclear fuel (NRC, 1993), but only licensed in the U.S. for storage (Greene et al., 2013). The TN-24 had a capacity of 24 PWR assemblies, and was designed to have a basket made of copper-plated borated 304 SS. There are no TN-24 casks in service, and it is not clear how the basket was to be assembled. The TN-24P differed from the TN-24 in several ways, including the use of aluminum-based neutron absorber plates. A single cask of the related TN-24P design is in use at Idaho National Laboratory; however, that design used aluminum-based neutron absorber plates.

TN-BRP Storage and Transport Cask – The TN-BRP cask is a storage and rail transport cask designed to accommodate 85 BWR used fuel assemblies. It was designed for one-time use, to transport 85 BWR fuel assemblies that were used at the Consumers Power Big Rock Point Plant from the DOE West Valley (NY) Demonstration Project to Idaho National Laboratory. Only one cask was built, and the transport Certificate of Compliance (71-9202) expired immediately upon completion of transport. The fuel basket of the cask was constructed of borated 304 stainless steel; manufacturing details are not available.

Yucca Mountain Project Transportation, Aging and Disposal Canister – Finally, the Transportation, Aging, and Disposal (TAD) canister design developed by the Yucca Mountain Project, for delivery of SNF to the repository site, on-site aging, and eventual disposal, was designed to use borated stainless steel plates as the neutron absorber materials for criticality control (DOE, 2008a). As part of their safety evaluation of the Yucca Mountain License Application, the NRC reviewed existing data on the properties and corrosion behavior of borated 304 SS, and concluded that it was appropriate for use in the TAD canister (NRC, 2014b).

Summary

Borated stainless steel has had limited use as a neutron absorber in dry storage canisters and casks (Greene et al., 2013). Two licensed canister designs, the FuelSolutions™ W74 and Transnuclear NUHOMS 52-B (a total of 34 canisters), use borated 304 SS plates as neutron absorber plates with carbon steel or stainless steel baskets; the borated stainless steel is not structural in either case. Three dry

storage or dual-purpose casks for uncanistered fuel have been designed to use borated stainless steel as a neutron absorber. Only the Castor V/21 is in commercial use, with 25 casks at the Surry Power Station. A single Transnuclear TN-BRP storage and transport cask was built, for one-time use to transfer a single load of spent fuel between two DOE sites. The Transnuclear TN-24 cask was designed but is not in use. Borated stainless steel was the design neutron absorber in the Yucca Mountain TAD canister (DOE, 2008a), and was accepted by the NRC in their evaluation of the Yucca Mountain License Application (NRC, 2014b).

Once in use, canisters and casks are commonly not opened, so the performance of borated steel as in dry storage canisters and casks has rarely been evaluated. However, a CASTOR V/21 cask at Idaho National Laboratory was opened 14 years after loading to assess the effects of long-term interim storage (NRC, 2001). The CASTOR V/21 basket is 304SS with integral welded borated 304 SS plates, and the inspection discovered that weld zones between 304SS and borated 304SS were foci for cracking, which apparently occurred during thermal testing prior to loading, but was not recognized at the time. This is consistent with experimental work showing that welding causes reduced ductility in borated 304 SS (Robino and Cieslak, 1997). As discussed in Appendix B, this effect can be mitigated by post-weld heat treatments.

Appendix D

Recommendations for Additional Corrosion Studies on Borated Stainless Steel

Limited experimental data exists on the corrosion of borated stainless steel under anoxic conditions. Experimental work is needed to identify the modes of corrosion, as well as to measure uniform corrosion rates for the borated stainless steel components in case of an early breach (penetration and flooding with groundwater) of both the overpack, and the stainless steel canister. The experimental testing program has to account for significant differences in geochemistry between different disposal environments (e.g. salt, crystalline, and argillaceous) and address the evolution of corrosion damage in these different geochemical settings.

The tests have to be designed to evaluate corrosion behavior for the container materials (borated stainless steel neutron absorbers) during the postclosure period. Following closure and backfill, the conditions are expected to be oxic for several years. Once all residual oxygen is consumed, the conditions will be anoxic in a low-permeability host media with backfill/buffer materials for the remainder of the repository performance period. Therefore, understanding the anaerobic corrosion rates and mechanisms for the materials of interest is critical.

Below we present a conceptual plan for additional experimental testing, which would be necessary to predict the realistic lifetime of a borated stainless steel component in a repository. This experimental plan is based on the experimental plan we have proposed for the austenitic stainless steels 304/304L and 316/316L (Ilgen et al., 2014).

Materials Selected for Testing

The test plan should include all eight borated stainless steel alloys (Types) specified under ASTM-A887-89. These alloys have to be Grade “A” alloys, as Grade “B” alloys are not proposed to be used in the standardized canisters. The exact geometry and thermal history of these samples (e.g. thicknesses, presence of welds and mechanically stressed zones) should be selected to represent the components within the standardized canister. Welding has been shown to cause significant impact on ductility, which can be restored to some degree if the welds are mitigated. However, there are no experimental results testing the corrosion of both as-welded and annealed welded materials. These should be given a priority, as they are a likely subject to localized corrosion.

Geochemical Systems and Geochemical Variables Selected for Testing

The geochemical conditions have to be selected to include several water compositions likely for each disposal concept (salt, granite, and clay/shale). Besides, the conditions are expected to depend on the failure scenario. For example, the composition of water entering the canister depends on whether the bentonite buffer is breached, and whether the groundwater has equilibrated with the bentonite buffer material.

Groundwater compositions for the laboratory testing are shown in Table B-1 (from Ilgen et al., 2014).

Table B-1. Proposed Representative Groundwater Chemical Compositions

Constituent		Shale		Granite	
		Shale-1	Shale-2	Granite-1	Granite-2
(mg L^{-1})	TDS	50,990	249,150	53,480	250,360
	Ca^{2+}	2,044	12,983	5,450	63,800
	Na^{+}	16,635	80,430	10,100	18,500
	Mg^{2+}	624.66	2,689	5,260	24
	K^{+}	215.11		57.6	371
	Cl^{-}	30,349	152,817	32,143	166,200
	Br^{-}			244	1,200
	SO_4^{2-}	996.97	207.97	<1	265
	HCO_3^{-}	340.25	24.13	54	0

Note: Granite data are from Frape et al. (2003); shale data are from Blondes et al. (2014).

The mode and rate of corrosion is controlled by moisture, pH, temperature, the presence of oxidizing species, and the concentrations of chloride and sulfide ions. Therefore, these variables have to be tested. Since borated stainless steel is a passive metal, special attention should be given to the performance of the passive Cr_2O_3 and NiO oxide layers under very reducing conditions in the presence of typical groundwater ions. Hydrogen embrittlement may be of concern, since corrosion of iron-based alloys under anoxic condition produces hydrogen. If the diffusion of hydrogen from the corroding surface is slow, this may result in hydrogen embrittlement of the surface and further enhance corrosion.

Corrosion rates of borated stainless steel have to be evaluated under both saturated (activity of water ~1) and unsaturated (only water vapor present) conditions to represent different failure scenarios. Therefore, we propose to evaluate corrosion of borated stainless steel at a constant temperature, while varying the activity of water, the aqueous matrix composition, in particular chloride and sulfide (or sulfate, if appropriate) concentrations, and also testing how the presence of water-saturated bentonite buffer affects the corrosion rates and corrosion products of borated stainless steel. Both general and localized corrosion have to be assessed.

Outcomes of the proposed laboratory testing program

The experimental testing program should be designed to address the following:

- General corrosion rates under anoxic conditions for borated stainless steels;
- Hydrogen embrittlement of the borated stainless steel components under diffusion-controlled conditions – if hydrogen gas is building up within the canister and the overpack – do we expect embrittlement and enhanced corrosion?
- Localized corrosion of the borated stainless steel under geochemical conditions representative of the salt, shale and granite repositories, and the extent to which localized corrosion may affect structural integrity of the component;
- Geochemical controls on the evolution of the passive film on the borated stainless steel under anoxic conditions.

Appendix E

Stress Corrosion Cracking of Spent Nuclear Fuel Interim Storage Canisters

Following initial cooling in pools, spent nuclear fuel (SNF) is transferred to dry storage casks for longer-term storage at the reactor sites. The storage cask systems are commonly welded stainless steel (Hanson et al., 2012) containers enclosed in ventilated concrete or steel overpacks. These cask systems are intended as interim storage until a permanent disposal site is developed, and until recently, were licensed for up to 20 years, and renewals also up to 20 years. In 2011, 10 CFR 72.42(a) was modified to allow for initial license periods of up to 40 years, and also, license extensions of up to 40 years. However, the United States does not currently have a disposal pathway for SNF, and these containers may be required to perform their waste isolation function for many decades beyond their original design criteria. Recent studies by the Nuclear Waste Technical Review Board (NWTRB, 2010), the Electric Power Research Institute (EPRI, 2011), the DOE Used Fuel Disposition Program (Hanson et al., 2012), and the Nuclear Regulatory Commission (NRC, 2012) have identified and prioritized potential concerns with respect to the safety performance of long-term interim storage. In each of these studies, the potential for canister failure by chloride-induced stress corrosion cracking (CISCC) was identified as the major concern with respect to canister performance.

Criteria for Stress Corrosion Cracking

Stress corrosion cracking is a localized corrosion phenomenon by which a through-wall crack could potentially form in a canister outer wall over time intervals that are shorter than possible dry storage times. In order for SCC to occur, three criteria must be met (Figure E-1): the metal must be susceptible to SCC, an aggressive environment must exist, and sufficient tensile stress must be present to support SCC. In general, these criteria are expected to be met, at least at some ISFSI sites, during the period of interim storage, especially if the development of a repository for final disposal is delayed. SCC of interim storage canisters has never been observed; however, that may be largely because detailed canister surface inspections for SCC have never been performed. Access to the canister surfaces through vents in the overpacks is extremely limited, and high surface radiation fields make removal of the canisters from the overpacks undesirable. Although efforts are currently in progress to develop the technologies to reliably detect SCC on in-service canisters, current risk assessments of

Aggressive Environment

The environment at any given location on the storage canister surface will be aggressive if the following two criteria are met: aqueous conditions must exist, and a corrosive chemical species must be present. The canister overpacks protect the canister from direct rainfall. Water may enter through the ventilation openings and be blown or drip onto the package, and evidence of this was seen during the recent canister surface inspections (Bryan and Enos, 2014; EPRI, 2014). However, any advective flow of water onto the packages is likely to be transient, and because the storage canisters are hot relative to outside temperatures, it will rapidly evaporate. Hence, persistent aqueous conditions are only anticipated to occur by deliquescence of salts in dust on the surface. For most dry cask storage systems, passive ventilation is utilized to cool the casks within the overpacks, and large volumes of outside air are drawn through the system. Dust and aerosols within the air are deposited on the steel canisters, and as the canisters cool over time, salts in the dust will deliquesce to form brine on the storage container surface. Deliquescence will occur when the relative humidity (RH) at the canister surface reaches a limiting value (RH_L) for corrosion; this value is generally somewhat lower than the deliquescence RH (RH_D) for the deposited salt assemblage.

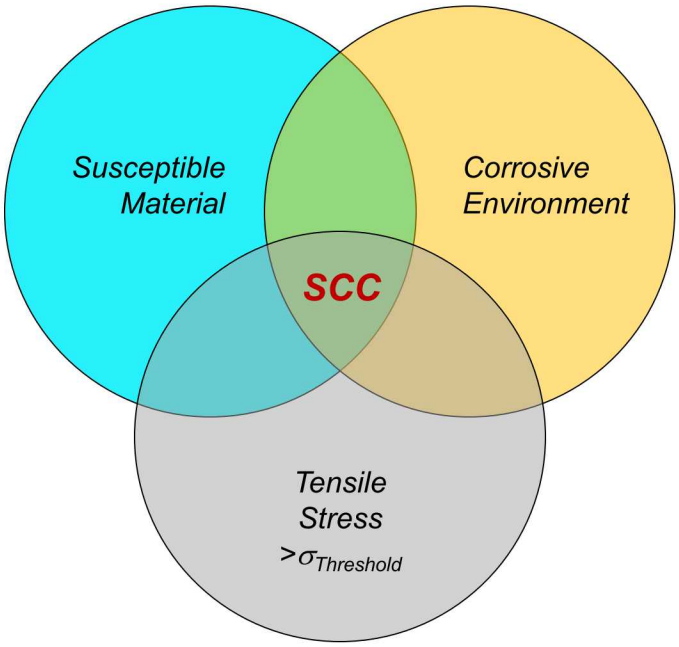

Figure E-1. Criteria for SCC initiation and growth.

The RH at the canister surface is controlled by the surface temperature at any given location, and the water content, or absolute humidity (AH) of the ambient air entering the overpack (Figure E-2). For typical conditions, it is anticipated that corrosion will not be possible until local canister surface temperatures drop below 60-70ºC. This does not indicate that newly-loaded canisters are safe from corrosion, however. Passive cooling by air advection through the overpacks is extremely effective and creates large temperature gradients on canister surfaces. For instance, surface temperatures measured on canisters at Diablo Canyon, containing high-burnup fuel only 2-4 years into storage, were as low as 50ºC near the inlets at the base of the canisters, although the temperature at the canister top was 150ºC (Bryan and Enos, 2014). Hence, even for hot, recently-loaded canisters, parts of the canister surface rapidly cool sufficiently to undergo deliquescence and, potentially, SCC.

Although other aggressive species may be present (e.g., high atmospheric concentrations of SO_2), the species that is considered to be aggressive for SCC is chloride. Many ISFSIs are located in coastal areas, where chloride-rich sea-salt aerosols may be deposited on the canisters. These deliquesce to form chloride-rich brines, and SCC is a well-documented mode of attack for austenitic stainless steels (including 304SS and 316SS) in marine environments (Kain, 1990). Recent canister surface inspections (Bryan and Enos, 2014; EPRI, 2014) have confirmed that chloride salts are present on the surface of in-service SNF storage canisters in near-marine settings (Figure E-3).

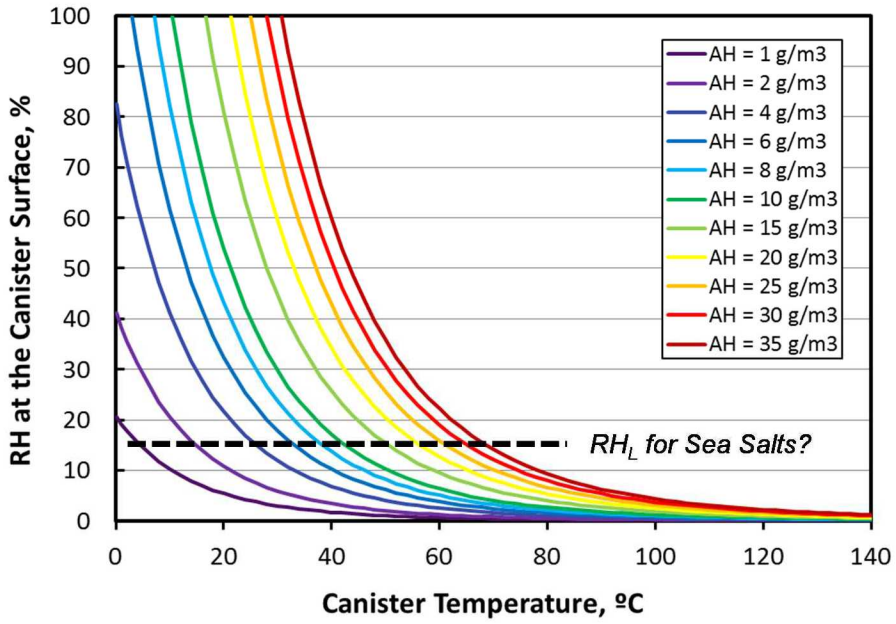

Figure E-2. Relationship between canister surface temperature, relative humidity, and RH at the canister surface.

A third potential criterion for a corrosive environment may be the amount of chloride present. Some studies have shown that there may be a lower limit on the amount of chloride on the package that can support SCC initiation—for instance, Shirai et al. (2011) determined experimentally that SCC could not initiate on 304SS, under conditions nominally representing atmospheric corrosion, at chloride loads <0.3 g/m^2. However, other work suggests that the lower limit of chloride loading for chloride-induced SCC, if there is one, is less than that value. Albores-Silva at al. (2011) observed SCC at chloride loadings of 0.1 g/m^2, and experimental studies by the US NRC (NRC, 2014a) showed that SCC could occur at sea salt loadings as low as 0.1 g/m^2 (0.056 g/m^2 chloride). Other studies (Tokiwai et al., 1985; Taylor, 1994; Fairweather et al., 2008) have shown that SCC corrosion may occur at loadings as low as 0.02 to 0.005 g/m^2. The United Kingdom Nuclear Decommissioning Authority has issued cautious operational limits for chloride surface concentrations on 316L waste packages of 0.01 g/m^2 for temperatures between 10 and 30°C and 0.001 g/m^2 for temperatures between 30 and 50°C (NDA, 2012). If there is a threshold chloride limit for SCC initiation, then it is apparently sufficiently low that it cannot be effectively used as a screening criterion for SCC.

It is likely that the rate and/or persistence of SCC growth is a function of the surface salt load, as it affects the current carrying capacity of the brine layer and the ability of the cathode, outside of the crack, to support corrosion at the anode, within the crack. This approach has been proposed for estimating maximum pitting penetration depths is several recent papers (for example, (Chen and Kelly, 2010; Krouse et al., 2014; Woldemedhin and Kelly, 2014), but has not been rigorously applied to SCC.

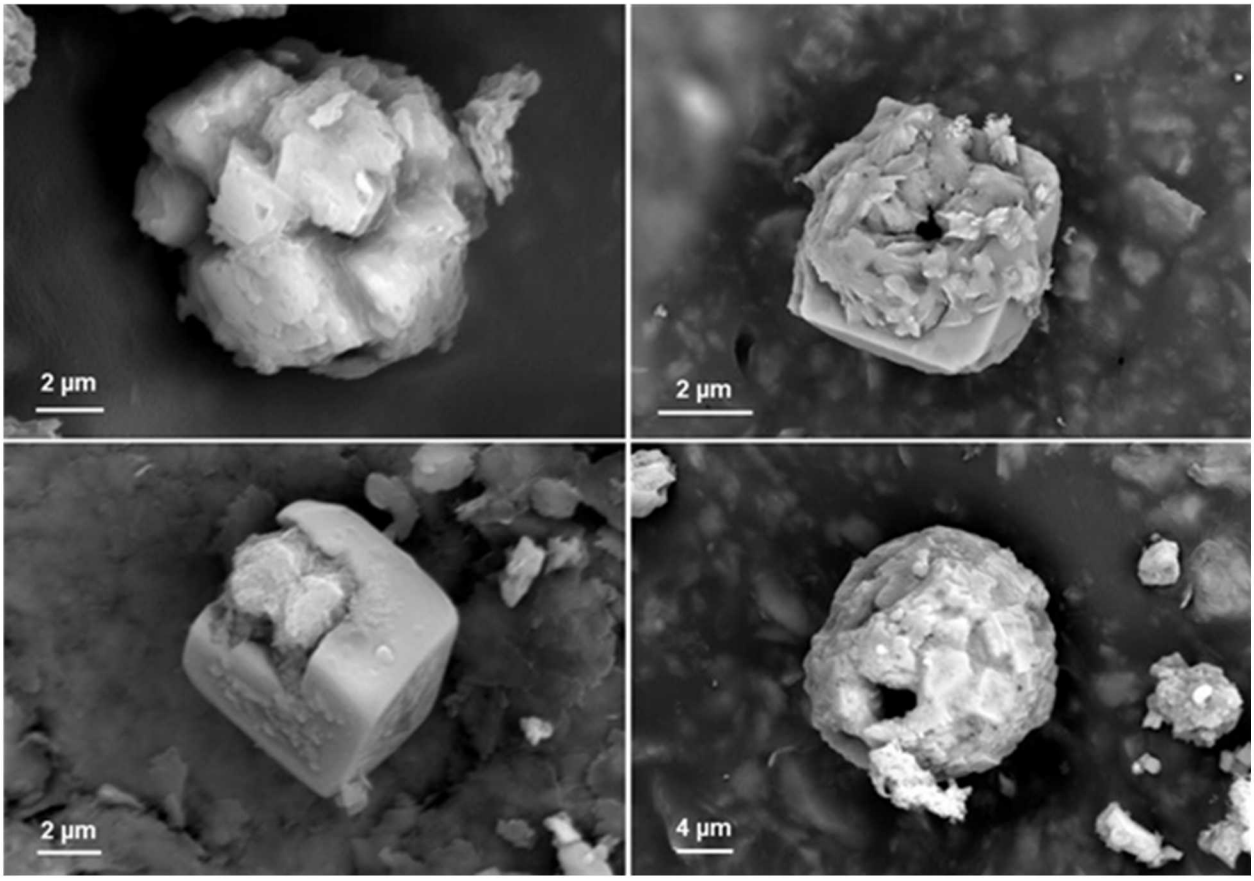

Figure E-3. Aggregates of sea-salts (NaCl + Mg-SO_4) collected from the surface of an in-service SNF storage canister at Diablo Canyon.

Although the potential for SCC is considered to be highest in near-marine environments, the very low threshold for SCC initiation means that inland sites cannot be considered immune. Chloride-rich salt aerosols may be generated by use of brackish water in cooling towers, or by salting of nearby roads during bad weather. The NRC applies a generic interim storage environmental impact statement (EIS) for all ISFSI sites, and does not accept that the risk of canister failure by SCC may be lower at inland sites. In defense of their generic interim storage EIS, the NRC has concluded that "…the impacts of continued storage will not vary significantly across sites; the impacts of continued storage at reactor sites, or at away-from-reactor sites, can be analyzed generically" (NRC Memorandum and Order CLI-14-08).

Material Susceptibility

The welded interim storage canisters are made of austenitic stainless steels, including 304/304L and 316/316L. These alloys are known to be susceptible to SCC in aggressive environments, should sufficient tensile stresses be present. SCC of 304/316 stainless steel has been observed in near-marine ambient temperature field tests and industrial sites (Kain, 1990; Hayashibara et al., 2008; Kosaki, 2008; Cook et al., 2011; Nakayama and Sakakibara, 2013; Cook et al., 2014). In elevated-temperature experimental tests with deliquesced sea-salts, meant to replicate conditions on the surface of a SNF interim dry storage canister, SCC has been shown to occur readily in both base metal and weld specimens (e.g., Nakayama, 2006; Prosek et al., 2009; Tani et al., 2009; Mintz et al., 2012; Prosek et al., 2014).

Although even base metal can undergo SCC in the presence of sufficient stress, there are several factors that can increase material susceptibility. These include the degree of sensitization, the degree of cold

working, the presence of iron contamination on the metal surface, and the surface finish (Parrott and Pitts, 2011).

Degree of Sensitization – When austenitic stainless steel is welded, the weld metal itself is melted and homogenized. However, with the heat-affected zone (HAZ) near the weld, the steel becomes sensitized. When the metal is heated during the welding process, Cr diffuses from the metal grains into the grain boundaries, where it combines with carbon to form chromium carbides. Sensitization results in the formation of chromium depleted zones at grain boundaries that facilitate the nucleation and propagation of localized corrosion such as pitting (often a precursor for SCC) and SCC. In general, the degree of sensitization induced by welding increases with the thickness of the welded material, because multiple weld passes are required and the heat input is greater. Increasing degrees of sensitization correspond to shorter incubation times prior to pitting and SCC initiation, formation of more pits and cracks, and more rapid pit and crack growth. Nakayama and Sakakibara (2013) estimate that the SCC initiation lifetime can decrease by more than an order of magnitude as the Ra increases from 0 to 20%, and crack growth rates can increase by a factor of 5, for atmospheric SCC conditions. Khatak et al. (1996) also saw increases in crack growth rates for sensitized 304SS, and noted that sensitization significantly lowered the threshold tensile stress for SCC, although this was for immersed conditions. The degree of sensitization has not been measured in representative storage canister welds, but it is likely that sensitization occurs, because of the metal thickness (5/8") and the multiple passes that are used to make the weld. Sandia National Laboratories (SNL) is currently in the process of procuring a full-diameter mockup of a storage canister, made using the same materials, weld schedules, and procedures as a NUHOMS storage canister. The mockup will provide prototypical welds that will be characterized with respect to weld residual stresses and degree of sensitization. This information will not be available until late 2015, however.

It should be noted that 304L stainless steel contains less carbon than 304 stainless, and hence, is much less susceptible to sensitization. Existing in-service storage canisters are made of either 304 or 304L; however, as steel fabrication techniques have improved, almost all modern 304 stainless steel is dual-certified, meaning that it not only meets the carbon content threshold for 304 (0.08 % maximum), but also the lower threshold for 304L (0.03 % maximum). Hence, sensitization is less of a factor for new canisters than for canisters made previously.

Degree of Cold Working – Cold working affects corrosion resistance of stainless steels (Khatak et al., 1996; García et al., 2001; Parrott and Pitts, 2011) for two reasons. First, it results in the formation of strain-induced martensite in the metal, which is less resistant to corrosion than austenite. Second, it induces local stresses and increases defect density; the dissolution rate of the metal is increased by the increased strain energy. The degree of cold working required to roll flat plates into cylindrical storage canister shells is not expected to significantly affect the corrosion resistance of the metal.

Iron Contamination – Contamination of the stainless steel surface with less corrosion-resistant forms of iron (e.g., tool steel or iron from support rails), will increase the likelihood of SCC, because the iron particles corrode more readily, supporting the development and stability of corrosive solutions (increased chloride concentrations and lowered pH) in pits and in SCC. It has been suggested that instances of SCC at temperatures below 60ºC are in many cases due to iron contamination on the stainless steel surface (Parrott and Pitts, 2011). This may be very important in some overpack designs: during the canister surface inspection at Calvert Cliffs, corrosion spots were observed on the canister surface, which were attributed to scratches and iron contamination from the rails (EPRI, 2014).

Surface Finish – A rough surface finish (>1 μm) can promote initiation of corrosion, apparently by trapping water and chloride ions on the surface (Parrott and Pitts, 2011). Also, surface grinding can also produce large local variations in stress, which may contribute by increasing strain energy and the dissolution rate of the metal. All storage canisters have rougher surfaces that 1 μm.

Crevice Corrosion – As with other factors that promote the development of the corrosive low-pH, high-chloride environment, the presence of crevices and crevice corrosion promotes initiation of SCC(Parrott and Pitts, 2011). There are many potential crevice locations in storage systems, with perhaps the most

important being the contact between the canister and the rail in horizontal storage systems, and contact between the canister and guide rails in vertical systems.

Tensile Stresses

In order for a SCC to form and grow, tensile stress is required. Residual stresses are imparted into the storage canister during manufacturing (rolling the steel plate to form a cylinder), and by welding. Although the residual stresses during cold-working have never been measured, it is anticipated that they will be too low to support stress corrosion cracking. However, residual tensile stresses related to the welding process are probably sufficient to support SCC, and may extent through the entire thickness of the shell. There have been no direct measurements of residual stresses associated with typical SNF dry storage canister welds; however, weld residual stress modeling for typical canister welds has been done by the NRC (2013). The through-wall stress profiles that the NRC predicted for circumferential and longitudinal canister welds are shown in Figure E-4. Results are shown for both isotropic and kinematic hardening laws; the two profiles are expected to bound the real stresses present in the weld regions. In the direction parallel to each weld, stresses throughout the wall thickness are tensile are greater than or equal to the yield strength of the metal. These tensile stresses are more than sufficient to support SCC, which would form perpendicular to the direction of highest tensile stress, or cutting across the weld region at right angles.

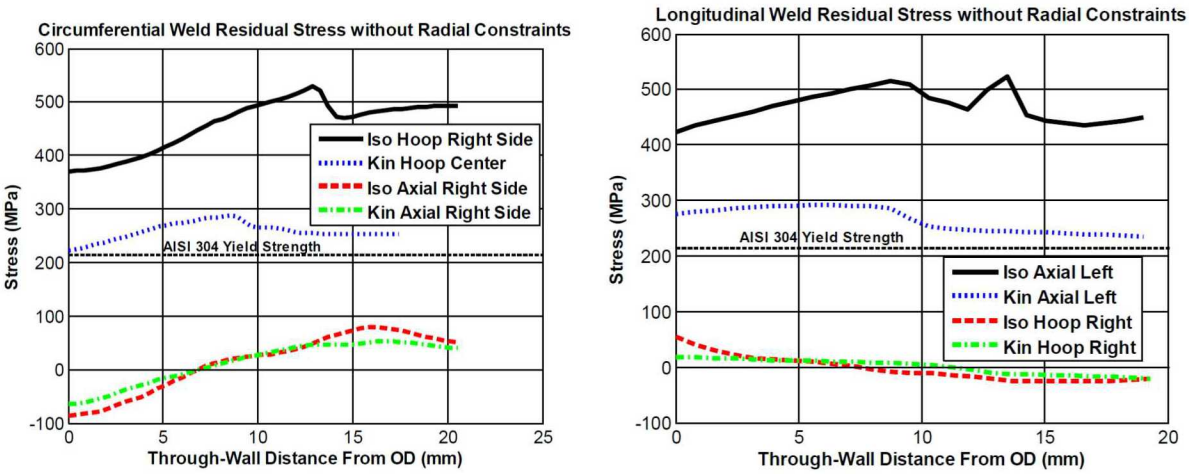

Figure E-4. Predicted weld residual stress profiles in canister weld regions (NRC 2013). Left-circumferential weld; right-longitudinal weld.

SCC initiation

As discussed above, the two of the three criteria that are required for stress corrosion cracking to occur, a a susceptible material, and the necessary tensile stress, are likely to be met by all storage canisters. It is less clear that a corrosive environment will exist at all storage sites, both inland and near-marine. However, the NRC does not currently accept environment as a potential mitigating factor with respect to SCC. Hence, it must be assumed that a corrosive environment will be present, and that SCC can and will initiate at all ISFSI sites. The time interval between SNF emplacement and SCC initiation—the SCC incubation time—is not known. As discussed previously, temperatures vary widely over the surface of canisters in storage overpacks, and even for canisters with high-burnup fuel, some fraction of the canister surface will be cool enough for deliquescence within several years of placement into storage. Once a deliquescent brine develops, localized corrosion (pitting) will initiate. The pits grow over time, and once

they reach a sufficient depth (generally around 70-100 μm, but this is a function of the tensile stresses present), they serve as initiation loci for SCC. Experimental studies have shown that SCC commonly originates at corrosion pits (for example, Kondo, 1989; Turnbull and Zhou, 2004; Nakayama, 2006; Turnbull et al., 2006b; Turnbull et al., 2006a; Kosaki, 2008; Prosek et al., 2009; Albores-Silva et al., 2011; Shirai et al., 2011). Pit growth rates are poorly understood; at ambient temperatures, pit growth may be quite slow (e.g., Chen and Kelly, 2010), and SCC initiation may take several years. However, experimental testing at even at moderately elevated temperatures (35º-60ºC), such as those expected on the canister surface for conditions of deliqscence, have resulted in pitting and SCC initiation within days to months (e.g., Prosek et al., 2009; NRC, 2014a). Therefore, it must be assumed that SCC initiation times will be short relative to the 150 year design lifetime of the standardized canister.

SCC Growth

In order for SCC to be a concern, crack growth rates must be sufficiently rapid to result in penetration of the canister wall, 0.5 to 0.625 inches thick within the designated design lifetime of 150 years. Stress corrosion crack growth rate is a function on many parameters, including temperature, magnitude of tensile stress, material properties such as yield strength and degree of sensitization, and environmental parameters such as chloride concentration (a function of RH), chloride surface load, and brine pH. A commonly-used form for the crack growth rate is provided below. It includes the effect of tensile stress in the form of the crack tip stress intensity factor (K), and temperature; environmental and material properties parameters are included implicitly by using relevant test data to develop the crack growth amplitude value (α_{crack}). A power law dependence is assumed for K, while an Arrhenius relationship is assumed for the temperature dependence (Wu and Modarres, 2012):

$$\frac{dx_{crack}}{dt} = \alpha_{crack} \cdot \exp\left[-\frac{Q}{R}\left(\frac{1}{T} - \frac{1}{T_{ref}}\right)\right] \cdot (K - K_{th})^{\beta_{crack}}$$

where:

dx_{crack}/dt is the crack growth rate
α_{crack} is the crack growth amplitude
Q is the activation energy for crack growth
R is the universal gas constant (8.314 J mol^{-1} K^{-1})
T is the temperature (K) of interest
T_{ref} is a reference temperature (K) at which α was derived
K is the crack tip stress intensity factor
K_{th} is the threshold stress intensity factor for SCC
β_{crack} is the stress intensity factor exponent.

The above equation is implemented in this report. For a cracked structure under remote or local loads, the stress intensity factor (K) is a measure of the stress field ahead of the crack. In elastic fracture mechanics, when the applied value of the stress intensity factor exceeds the material's critical value, crack advance occurs. For subcritical cracking, the process of crack advance is linked to the applied value of the stress intensity factor through curve fits that are based on extensive experimental data. The stress intensity factor K is defined as (Wu and Modarres, 2012):

$$K = \sigma_{applied} Y \sqrt{\pi x_{crack}}$$

where

$\sigma_{applied}$ is the tensile stress,

Y is a shape parameter, equal to 1 for an infinite flat plate. Given that the waste canister circumference and length are much greater than the thickness of the canister wall and the crack depth/length at the time of penetration, this is a reasonable approximation.

x_{crack} is the crack depth.

Because the crack growth rate is a function of temperature, the elevated temperatures on the canister surface will result in faster crack growth rates. A summary of crack growth rate experimental data, collected for stainless steels exposed to deliquescent sea salts at a range of temperatures, is shown in Figure E-5. All of these data were collected specifically to address the issue of SNF dry storage canister corrosion. Data include rates from both 304 and 316 stainless steel, and include base metal, weld, and sensitized samples (Hayashibara et al., 2008; Kosaki, 2008; Tani et al., 2009; Cook et al., 2011; Shirai et al., 2011; Nakayama and Sakakibara, 2013). There is a good deal of scatter in the measured rates, and some of the more rapid rates may not be relevant to thick metal samples (Shirai et al., 2011). However, it is apparent that, at elevated temperatures, penetration could occur within 150 years even at the slowest rates measured. Penetration rates at ambient temperatures are much slower, but penetration is still possible within 150 years.

Summary

On the basis of the available data, the three criteria for SCC are likely to be met on SNF canister surfaces during storage at least at some sites. SCC is likely to initiate within the 150 year design lifetime of the canisters, and may penetrate the canister walls. A standardized canister design must address the concerns for SCC and be designed to mitigate this risk. Possible solutions include building the canister out of materials that are less susceptible to SCC, such as duplex stainless steels. However, 304L and 316L are acceptable materials, so long as steps are taken to reduce susceptibility to SCC by performing weld mitigation. Possible mitigation techniques include high temperature thermal annealing of the entire canister prior to loading, which would both remove highly tensile weld residual stresses and eliminate the effects of sensitization by re-dissolving the Cr-rich carbides back into the metal. Alternatively, mitigation of weld residual stresses could be done using techniques such as shot peening, laser peening, or low plasticity burnishing. These techniques create a thin layer of metal on the surface of the treated region that has high compressive stresses, preventing initiation of SCC.

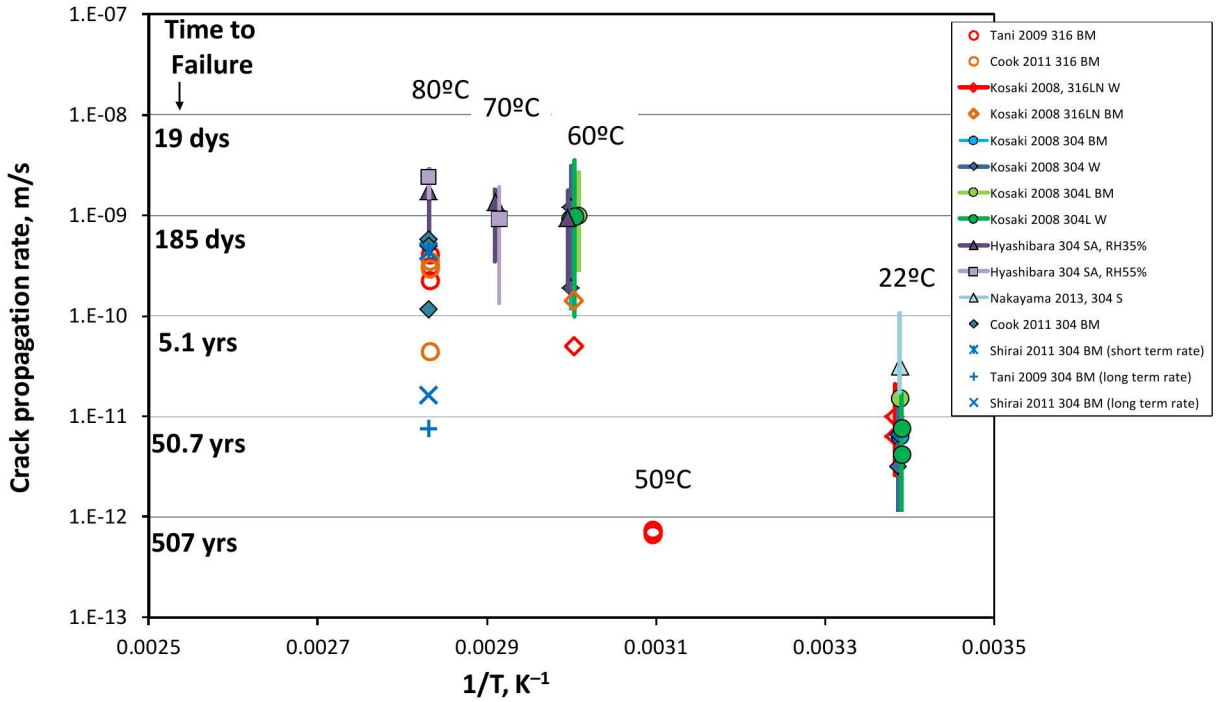

Figure E-5. SCC propagation rates for atmospheric corrosion of 304SS and 316SS. BM –base metal; W–weld sample; SA–solution annealed; S–sensitized. Bars represent reported ranges (if more than one), while symbols represent average values. Time to failure corresponds to the time required to penetrate a 0.625” thick canister wall.

Appendix F

Generic Case for Postclosure Safety of STAD Canisters

Following initial cooling in pools, spent nuclear fuel (SNF) is transferred to dry storage casks for longer-term storage at the reactor sites. The storage cask systems are commonly welded stainless steel

Introduction

Disposability of STAD canisters can be demonstrated with a safety case that includes screening of features, events and processes (FEPs), and a performance assessment for comparison to regulatory postclosure dose standards. This is the basic set of analyses needed for licensing repository postclosure performance, and it has been performed twice in the U.S. using site-specific information (DOE, 1996; DOE, 2008b). The difference with demonstrating STAD canister postclosure performance presently in the U.S. is that without a repository site the analyses must be generic, and generic repository safety analysis has never before been subject to licensing review.

Fortunately the STAD canister will be only one part of a multi-barrier disposal system, so that other barriers can be relied on for waste isolation from the biosphere. A previous license application (DOE, 2008b) assigned no containment function to the spent fuel canister, because such functions were performed by the waste form, waste package, engineered barriers, and natural barriers. The canister contributed to other types of performance such as structural integrity of the waste package.

This appendix presents a brief survey of generic performance assessment analyses for crystalline, clay/shale, and salt host media. It refers to a previous generic safety case study (Freeze et al., 2013) for model description and rationale, and FEP screening. This survey shows how simple models could be used to establish reasonable assurance that the STAD canister would perform, along with other barriers, in a manner that meets regulatory performance standards.

As noted in Section 3.1.5 there is a possibility that the neutron absorber plates in STAD canisters could fail to perform their function in the event of waste package breach, and exposure to ground water for fewer than 10,000 years. Understanding the potential for postclosure criticality, and the effects of a criticality event if one occurs, are the key challenges for demonstrating STAD canister disposability. This appendix addresses criticality potential for the various host media: salt, unsaturated hard rock, and saturated crystalline or clay/shale media. The discussion includes specific proposals for the types of analysis that could be used for generic demonstration of postclosure criticality control.

Postclosure Waste Isolation

Waste isolation performance was analyzed for generic salt, crystalline and clay/shale media (Freeze et al., 2013). The basic conceptual model of the disposal system was the same (Figure F-1). The simplicity of the models means they have few parameters and can be readily adapted to site-specific analysis. For two of the three models (salt and clay/shale), waste package containment (including the canister) was neglected because isolation could be provided by the natural barriers and slowly dissolving waste form (Figures F-2 and F-3). For the crystalline rock model containment was assigned to the disposal overpack and not the fuel canister, and 1% of the overpacks were assumed to fail (Figure F-4). In each case the calculated dose meets a 15 mrem yr^{-1} dose standard for the first 10,000 years, and 100 mrem yr^{-1} after that. For the unsaturated hard rock repository, extensive performance assessment analysis was demonstrated using site-specific information (DOE, 2008b).

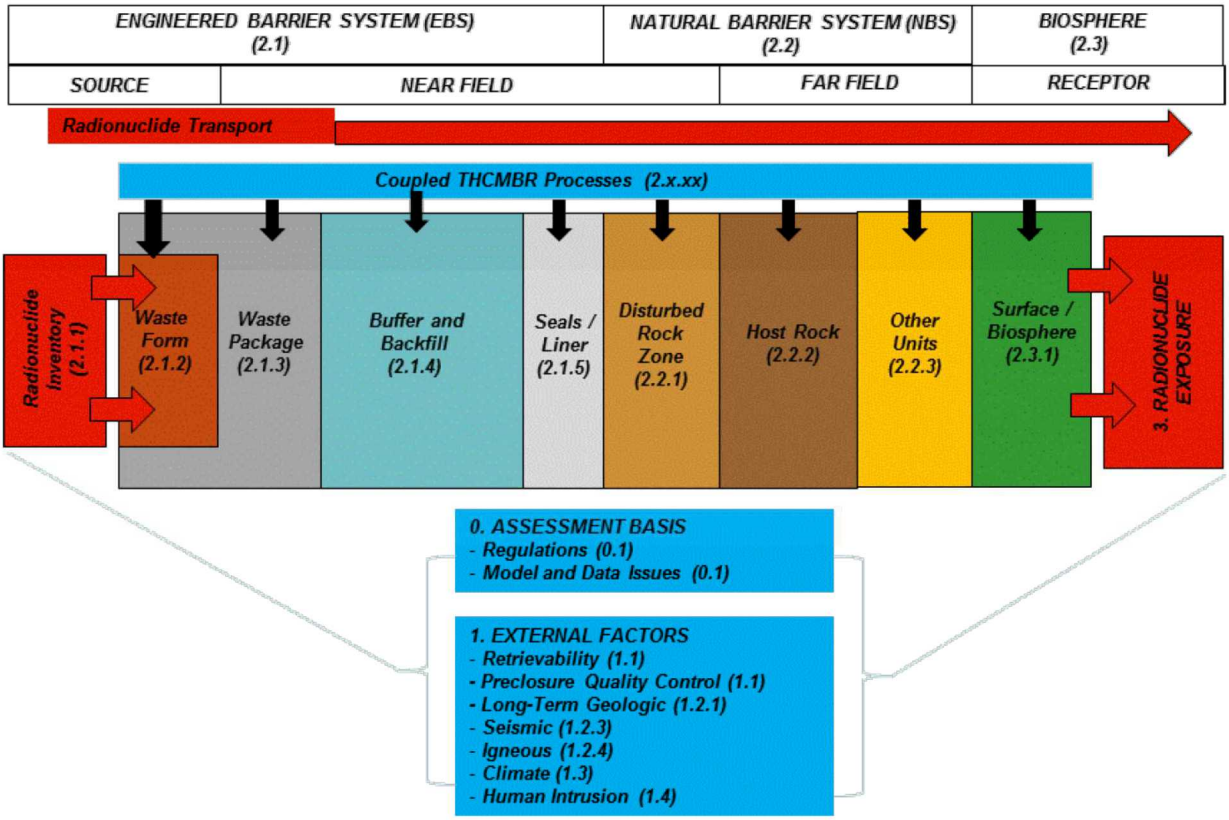

Figure F-1. Conceptual model for generic repository waste isolation analysis (after Freeze et al., 2013).

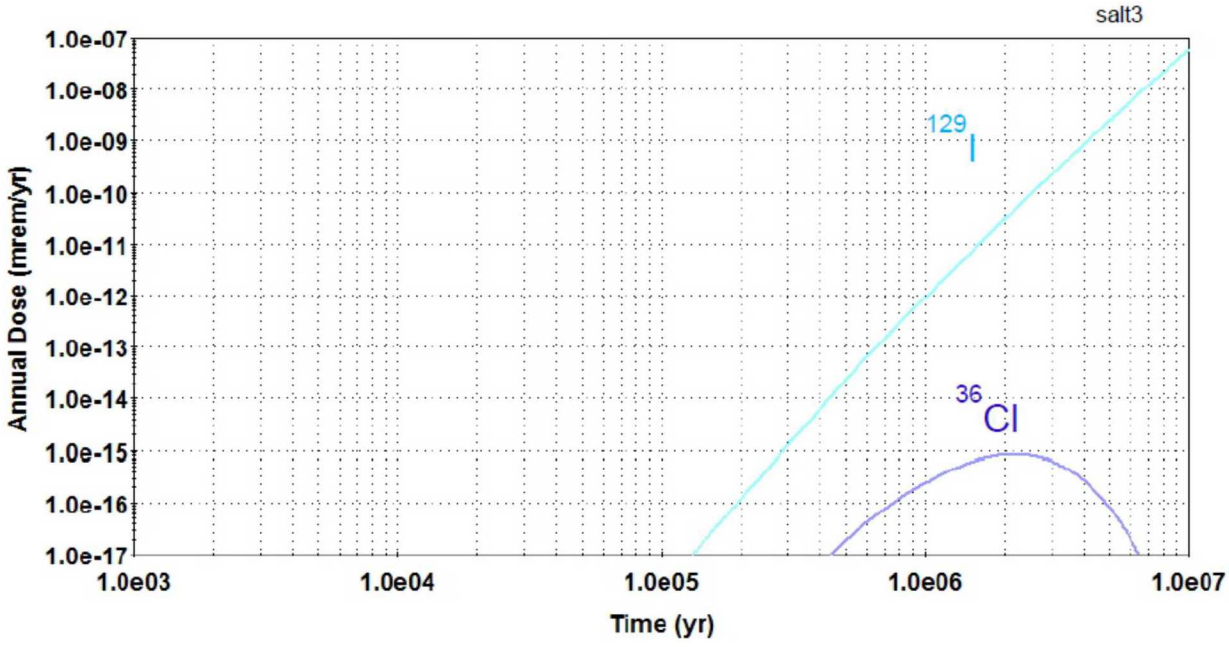

Figure F-2. Calculated dose for a generic salt repository (after Freeze et al., 2013).

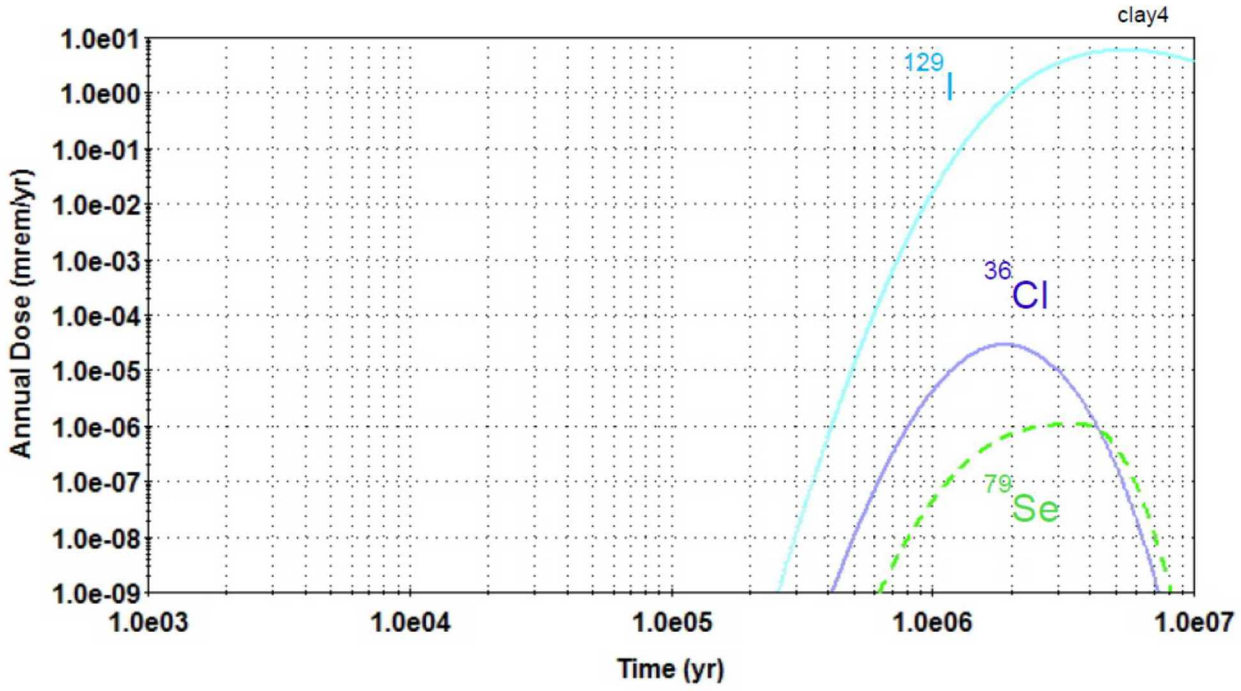

Figure F-3. Calculated dose for a generic clay/shale repository (after Freeze et al., 2013).

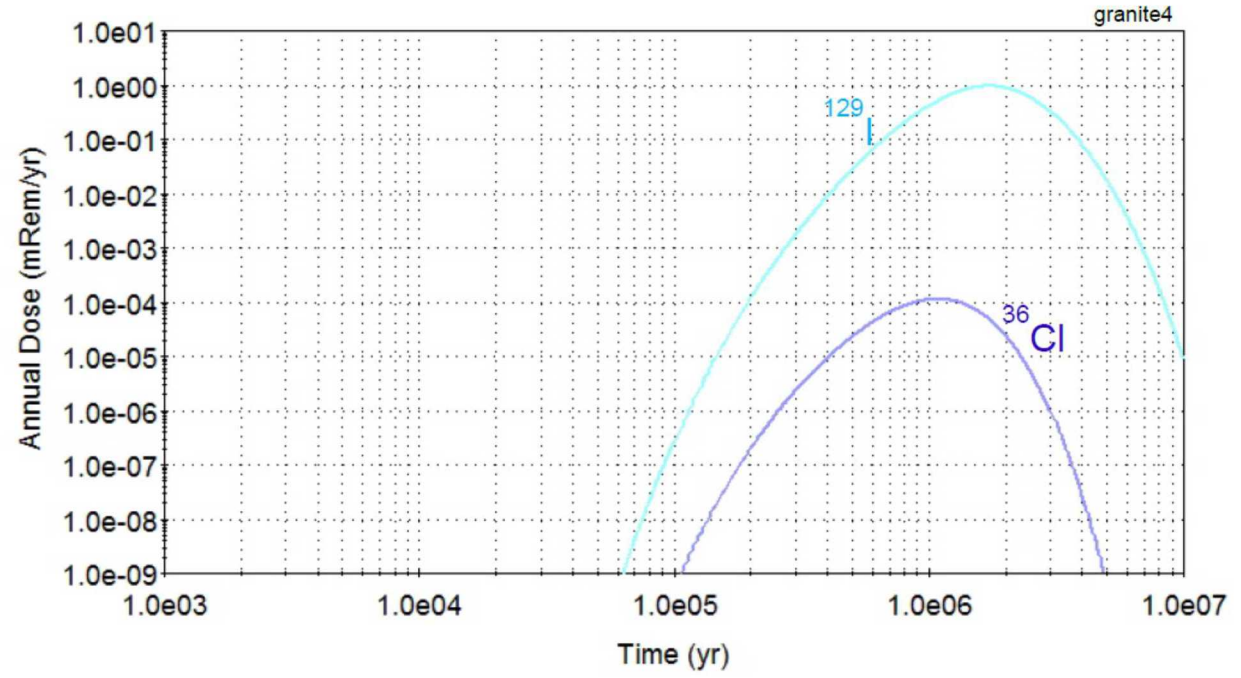

Figure F-4. Calculated dose for a generic crystalline rock repository (after Freeze et al., 2013).

Postclosure Criticality Control

For postclosure criticality to be excluded from performance assessment based on low probability, the aggregate probability must be less than 10^{-4} over 10,000 years (Table F-1). Thus, the circumstances leading to waste package breach, flooding, and degradation of neutron absorbers (or degradation of basket structure) must have aggregated probability less than 10^{-4}. For disposal environments with potential to flood a breached package with fresh water (not saline or unsaturated), this analysis assumes: 1) the disposal overpack is designed and manufactured to provide reasonably high-reliability containment for at least 10,000 years; and 2) the combined effects from the geologic setting and engineered barriers lower the probability of disruptive events leading to waste package failure, to less than 10^{-4} for 10,000 years. Seismicity and faulting may be the most likely disruptive events for geologic settings, and the latter assumption relies on relatively quiescent tectonics, and the dampening effect of backfill. This discussion of postclosure criticality is provided because the degradation rate for borated stainless steel (recommended material for neutron absorber plates) is uncertain, and could be large enough that complete degradation (leaving less than the minimum thickness to prevent criticality) is possible.

A potentially important event leading to waste package breach is "early failure" due to manufacturing defects. Previous analysis estimated the mean probability of an early-failure condition at $4x10^{-5}$ for waste packages, and $4x10^{-7}$ for drip shields (SNL, 2007a). The joint probability for early failure of a specific waste package and its drip shield is clearly less than 10^{-8}, but the probability of either type of failure was included in performance assessment (DOE, 2008b). The previous analysis was thorough and the prospect for significant reduction in early failure probability is limited (review of the analysis is currently underway and will be reported in FCRD-UFD-2015-000714 and FCRD-UFD-2015-000129). However, reduction may be possible through improvements in the way manufacturing defects are represented in performance assessment, for example, through impacts on the overpack corrosion rate rather than assigning an initial breach condition. Early failure is therefore likely to be part of any performance assessment, and for robust waste packages it may be the most probable mode of failure in 10,000 years. In the event of waste package breach due to manufacturing defects, the event sequence possibly leading to criticality will involve other uncertainties that reduce the aggregate probability as discussed below.

Another potentially important event sequence begins with inadvertent human intrusion by drilling into a waste package. The human intrusion standard (defined for a 10,000-year stylized scenario by 10CFR63 and 40CFR197) involves larger threshold screening probabilities than individual protection standards (Table F-1) but the effects of human intrusion on the potential for criticality must still be considered. A waste package breach caused by human intrusion could have the same long-term effect on neutron absorber materials as a breach due to manufacturing defects. Possible linkage between human intrusion and criticality is also discussed below.

Postclosure Criticality in a Salt Repository – Certain neutronic calculations performed evaluating the feasibility of direct disposal of dual-purpose canisters (most of which have readily degraded, aluminum based absorbers), are applicable to STAD canisters. In particular, a high-reactivity model was formulated to study the effect of flooding ground waters of different composition (Hardin et al., 2014). The model and results for sodium chloride brine over a range of concentration, are shown in Figure F-5. Whereas a saturated NaCl at 20°C has a concentration of approximately 6 molal, or 158,000 ppm chloride by the method used for this calculation, substantial reduction in reactivity is shown for concentrations half this value especially for higher burnup. This results because natural chlorine has an isotopic fraction of 75% ^{35}Cl, a neutron absorber.

In a salt repository there is very little free water or brine, under normal conditions. Disposal concepts for salt typically call for heavy waste packages from low-alloy steel, which corrodes on contact with water, reacting to form gaseous hydrogen. With little water present, waste package corrosion will be very slow, and there is little possibility for flooding even if waste package breach occurs from corrosion. Should flooding occur, naturally occurring waters in the salt formation will be brines. Waste package breach due

to manufacturing defects is insignificant in this environment. Human intrusion may occur but the drill must penetrate the robust waste package, and the drilling fluid typically used in evaporites is saturated brine. Hence, there is little potential for criticality to occur in a salt repository.

Postclosure Criticality in an Unsaturated, Hard-Rock Repository – The STAD canister described in the performance specification is based on the transport-aging-disposal (TAD) canister (DOE, 2008b). The performance of that canister in an unsaturated, hard-rock repository was analyzed extensively and reviewed by the U.S. NRC, resulting in a Safety Evaluation Report (NRC, 2014b). The review concurred that borated stainless steel, in combination with other engineered features and the unsaturated natural setting, would function as intended to prevent criticality for at least 10,000 years, in the event of early failure or other waste package breach.

Postclosure Criticality in Other Host Media – The crystalline rock and clay/shale disposal concepts call for packaging in corrosion resistant overpacks (Hardin and Kalinina, 2015). Like the Swedish KBS-3 concept (SKB, 2011), clay-based material would surround and condition the corrosion environment at the waste package surface. The result could be a high-reliability containment envelope, for which manufacturing defects could be minimized using modern methods of inspection and testing. As an extreme example, "early failure" could definitely be excluded from consideration if two or more independent, corrosion resistant containment barriers were used (i.e., joint probability $< 10^{-8}$ per year).

In addition to a high-reliability overpack, realistic representation of other processes provides additional reduction in criticality probability (Figure F-6). The time to breach may consume a significant portion of the 10,000-year performance period. Flooding of the STAD canister after package breach is not definite, because the canister itself must also fail from corrosion, and the source of water must be sufficient to flood the canister (e.g., if water must flow through a hydrated clay backfill, and then through a small breach). Once ground water enters a STAD canister, the borated stainless steel absorber plates must substantially corrode to allow the possibility of criticality (at corrosion rates discussed elsewhere in this report). Even with substantial or complete degradation of absorber plates, as-loaded burnup analysis of fuel canisters shows that many have available uncredited reactivity margin. Other effects also come into play such as the salinity of ground water, and the probability of a fuel mis-load (which could either increase or decrease canister reactivity).

The same type of argument can be made for criticality as a consequence of human intrusion (Figure F-7). Drilling equipment used for clay/shale media is typically not configured for penetrating heavy metal containers (e.g., 5 cm wall thickness). Even if penetration occurs and the STAD canister fills with drilling fluid or ground water, the absorber plates may corrode slowly, and the as-loaded configuration of the canister may be sub-critical.

Table F-1. Summary of Postclosure Dose Standards Based on 10 CFR Part 63.

FEP probability (per year)	**Individual protection standard 15 mrem yr^{-1} for 10,000 yr** **63.311(a)(1)**	**Individual protection standard 100 mrem yr^{-1} after 10,000 yr** **63.311(a)(2)****	**Individual protection standard for stylized human intrusion 15 mrem yr^{-1} for 10,000 yr** **63.321(b)(1)**	**Individual protection standard for stylized human intrusion 100 mrem yr^{-1} after 10,000 yr** **63.321(b)(2)****	**Groundwater protection standard limits on: combined ^{226}Ra and ^{228}Ra activity; gross α activity; dose from combined β and photon emitting radionuclides; for 10,000 yr** **63.331**
$< 10^{-8}$ *	Not Included 63.342(a)	Not included 63.342(c)	Not included 63.342(a)	Not included 63.342(c)(1)	Not included 63.342(a)
$10^{-8} < p < 10^{-5}$	Included	Included	Not included 63.342(b)	Not included 63.342(c)(1)	Not included 63.342(b)
$> 10^{-5}$	Included	Included	Included	Included	Included

* If the probability of a feature, event, or process (FEP) is greater than 1 x 10^{-8} per year, the FEP can also be excluded if its effect on repository performance (however probable) can be demonstrated to be not significant. (10 CFR 63.342(a))

** For these two standards, 10 CFR 63.342(c) requires the inclusion of seismic and igneous activity, subject to probability limits, and also requires inclusion of the effects of climate change (with prescribed limits on the effects of climate change) as well as inclusion of the effects of general corrosion.

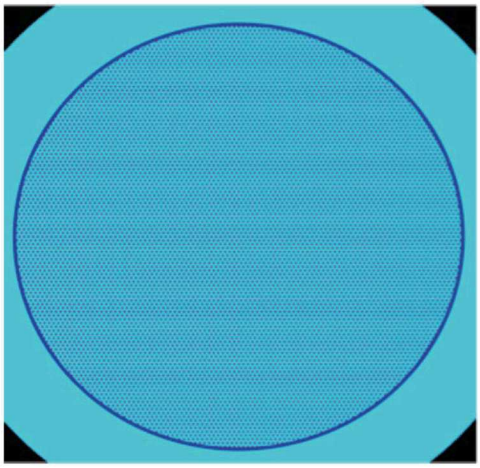

High-reactivity model with PWR fuel rods uniformly distributed, and no basket structure or neutron absorbers.

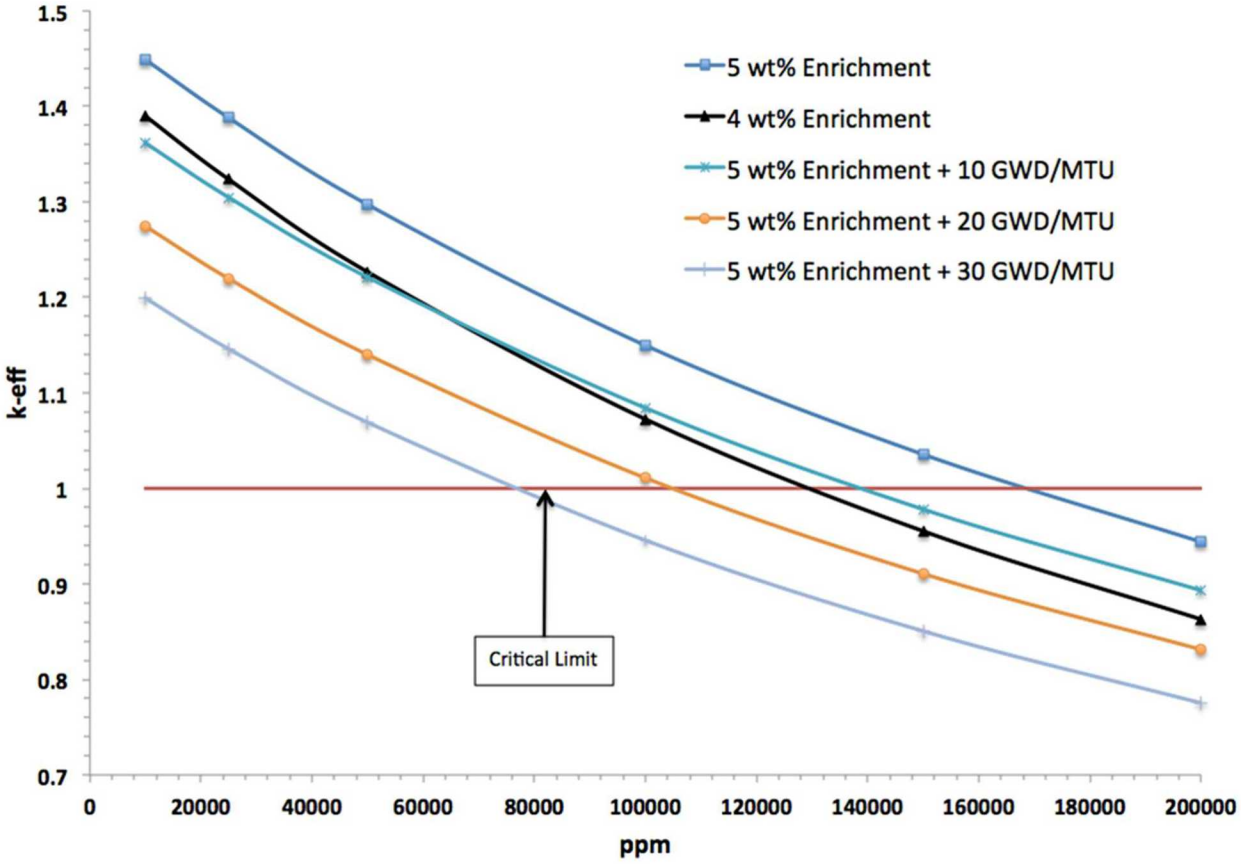

Note: Concentration of 158,000 ppm chloride corresponds to a saturated salt brine (6 molal) at 20°C.

Figure F-5. High-reactivity model geometry (upper) and neutron multiplication factor (k_{eff}) as a function of NaCl salt concentration, for different fuel types (lower).

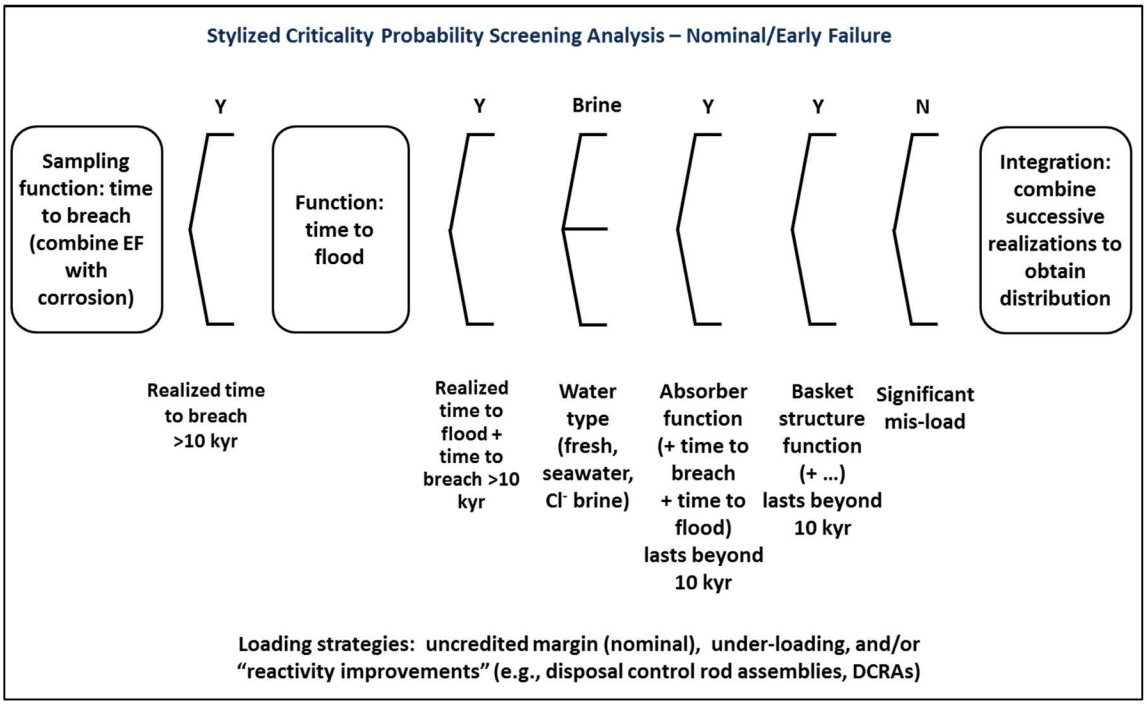

Figure F-6. Event-tree logic for a stylized criticality screening analysis.

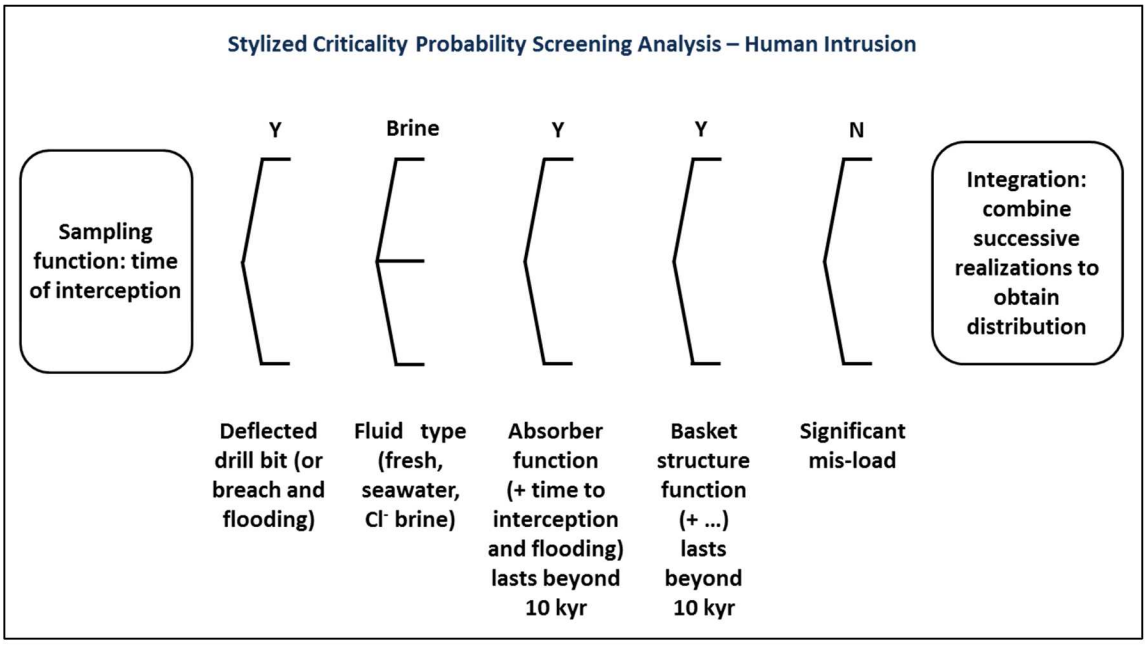

Figure F-7. Event-tree logic for a stylized criticality screening analysis of the inadvertent human intrusion scenario.